

Article

Sprayed-Polyurea-Modified Asphalt: Optimal Preparation Parameters, Rheological Properties and Thermal Properties

Qinyuan Peng ¹, Xiaolong Sun ^{1,2,*}, Zhisheng Liu ³, Jiao Jin ⁴ , Huayang Yu ⁵ and Yingmei Yin ¹

¹ School of Civil and Transportation Engineering, Guangdong University of Technology, Guangzhou 510006, China

² Highway Engineering Key Laboratory of Sichuan Province, Southwest Jiaotong University, Chengdu 611756, China

³ The Key Laboratory of Road and Traffic Engineering, Ministry of Education, Tongji University, Shanghai 201804, China

⁴ School of Traffic and Transportation Engineering, Changsha University of Science and Technology, Changsha 410114, China

⁵ School of Civil Engineering and Transportation, South China University of Technology, Guangzhou 510641, China

* Correspondence: xls1998@gdut.edu.cn

Abstract: For promoting modifying application of sprayed polyurea (SPUA) in asphalt pavement materials, the effects of sprayed polyurea materials on high-temperature and fatigue performance of asphalt binders were investigated from different aspects. First, the optimal preparation parameters of sprayed-polyurea-modified asphalt binders (SPMAs) were determined by designing an orthogonal test. Then, the high-temperature and fatigue properties of sprayed-polyurea-modified asphalt binders with different contents were characterized by rheological testing methods, including Brookfield rotary viscosity (RV) test, performance grading (PG) test, multiple stress creep recover (MSCR) test, linear amplitude sweep (LAS) test and time sweeping (TS) test. Finally, the thermal properties of the asphalt binders were analyzed by differential scanning calorimetry (DSC) test. The results showed that the optimum preparation parameters were determined by the extreme difference analysis method and analysis of variance (ANOVA) method, and the shearing time was 40 min, the shearing rate was 6000 rpm and the shearing temperature was 150 °C. Sprayed polyurea positively affected high-temperature performance of asphalt binders and could improve fatigue resistance of asphalt binders. Moreover, the Brookfield rotary viscosity test, multiple stress creep recover test and linear amplitude sweep test had high sensitivity to the performance of sprayed-polyurea-modified asphalt binder, which could help to distinguish the effect of sprayed polyurea dosing on performance of asphalt binders accurately. The differential scanning calorimetry test showed that sprayed polyurea was beneficial to high-temperature stability of asphalt binders, which explains the reason why sprayed-polyurea-modified asphalt binders have excellent high-temperature performance from a microscopic perspective.

Keywords: modified asphalt binder; sprayed polyurea resin; high-temperature property; fatigue property; thermal property; correlation



Citation: Peng, Q.; Sun, X.; Liu, Z.; Jin, J.; Yu, H.; Yin, Y.

Sprayed-Polyurea-Modified Asphalt: Optimal Preparation Parameters, Rheological Properties and Thermal Properties. *Coatings* **2023**, *13*, 544. <https://doi.org/10.3390/coatings13030544>

Academic Editor: Valeria Vignali

Received: 3 February 2023

Revised: 23 February 2023

Accepted: 25 February 2023

Published: 2 March 2023



Copyright: © 2023 by the authors. Licensee MDPI, Basel, Switzerland. This article is an open access article distributed under the terms and conditions of the Creative Commons Attribution (CC BY) license (<https://creativecommons.org/licenses/by/4.0/>).

1. Introduction

Compared with cement concrete pavement, asphalt pavement has advantages of short maintenance cycle, easy maintenance and good driving performance and has gradually replaced cement concrete pavement and become the main application of pavement structure [1–4]. However, it has been found in practical applications and research that common asphalt materials are prone to deformation under prolonged or excessive loading and performance degradation under light, high and low temperatures and rain, resulting in shortened lifespan of asphalt pavements [1]. The available research results show that polymer modification technology is an effective way to improve performance of asphalt

binders [2]. However, while polymers improve performance of asphalt binders, they also add other new problems. For example, the excellent high- and low-temperature performance of SBS-modified asphalt binder is favored by researchers, but its high cost and poor compatibility limit application in low- and medium-grade pavements [5,6]. Ethylene-vinyl acetate copolymer, polyethylene and other modified asphalt both have good high-temperature performance and economy, but low-temperature performance is difficult to meet expectations [7–10]. For this reason, researchers are still searching for modifiers with good modification effects [11,12]. This paper investigated the effect of a high-performance resin material, SPUA, on high-temperature performance and fatigue performance of asphalt binders. SPUA is a kind of polymer material containing urea bonds, carbamate and other functional groups [13]. After curing, SPUA has extremely high tensile strength, impact strength, waterproofing, anti-corrosion and wear resistance and other excellent properties. It has been widely used in many fields, such as the military industry, coating, waterproofing, anticorrosion and engineering construction [14–16]. However, in the asphalt road field, fewer researchers are studying the preparation method and modification effect of SPMA. It is well known if the modification effect is excellent determines whether the modified material can be widely used in practical engineering. Therefore, it is necessary to conduct research on the road performance aspects of SPMA, evaluate the applicability of SPUA to asphalt binders and provide a relevant basis for research, application and promotion of SPUA in asphalt pavements.

High-temperature performance and fatigue performance of asphalt binders have been the focus of researchers in response to the progressively harsher high-temperature environment and increasing traffic volume [17–21]. Many complete and mature test methods and evaluation systems have been developed for high-temperature performance of asphalt binders. Among them, due to their higher sensitivity, accuracy and precision, rheological-based testing methods have gradually become mainstream, for example, the PG test, MSCR test, zero shear viscosity test (ZSV), elastic viscosity index, frequency sweeping, etc. [22,23]. For fatigue resistance performance of asphalt binders, the main indicators include fatigue factor ($|G^*| \sin \delta$), damage factor ($\tan \delta$) and fatigue life based on the TS test and LAS test. However, $|G^*| \cdot \sin \delta$ and $\tan \delta$ are fatigue performance parameters obtained in low loading times and linear viscoelastic range, but these two indicators lack relevance with actual fatigue performance of asphalt pavements [24–26].

In summary, researchers have proposed many relevant indicators for high-temperature performance and fatigue resistance of asphalt binders. However, due to the different loading methods and calculation principles between the tests, there are different degrees of difference among the indicators, which affects evaluation of real performance of asphalt binders [17,26,27]. Therefore, to accurately evaluate degree of influence of SPUA on asphalt binders, it is necessary to analyze applicability of different performance indicators to SPMA.

The main objective of this study focused on the optimal preparation process parameters, high-temperature performance and fatigue performance evaluation of SPMA. First, the optimum preparation process parameters of SPMA were determined based on orthogonal test combined with range analysis and variance analysis. On this basis, the high-temperature performance and fatigue resistance of SPMA with different contents were studied. Among them, the high-temperature performance characterization methods include PG test and MSCR test, and the fatigue resistance test includes LAS test and TS test. Finally, the applicability of different indicators to the performance evaluation of SPMA was investigated by correlation analysis.

2. Materials, Preparation and Test Methods

2.1. Materials

2.1.1. Asphalt Binder

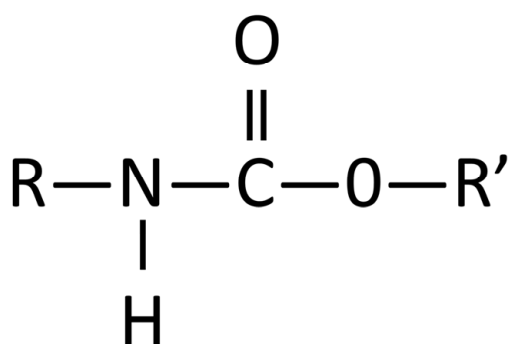
The base asphalt binder used in this paper was 70# base asphalt binder (Kunlun brand, Petrochina Fuel Oil Co., Ltd., Zhuhai, China), and its main performance indicators are listed in Table 1.

Table 1. Properties of base asphalt binder.

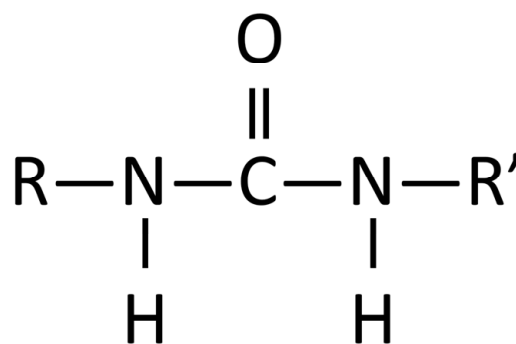
Properties	Unit	Test Result	Specification
Performance grade	°C	64	ASTM D7643-10
Softening point	°C	46.25	ASTM D36
Ductility (10 °C)	cm	60	ASTM D113
Penetration (25 °C)	0.1 mm	65	ASTM D5
Dynamic viscosity (60 °C)	Pa·s	218	ASTM D2170
Mass variation	%	−0.114	ASTM D2872
After TRTOF Aging Penetration ratio	%	≥81	ASTM D5
Ductility (10 °C)	cm	≥6	ASTM D113

2.1.2. SPUA Base Material

The modifier used in this paper is sprayed polyurea (SPUA), a high-performance resin material containing many strong polar functional groups: urea bonds and carbamate [10]. Figure 1 shows the molecular formulas of urea bond and carbamate. The technical indicators of SPUA are shown in Table 2. In this study, we expect to process the SPUA base material to a suitable size by grinding it and applying it in asphalt binders. However, during the grinding process, it was found that the excellent stress absorption properties of SPUA at normal temperature greatly deteriorated the efficiency of the grinding machine. Therefore, this study took advantage of the high brittleness of the polymer at the glass transition temperature to grind the SPUA base material in a low-temperature environment. Figure 2 showed the particle size distribution of the SPUA modifier after grinding. The solid red line shows the volume proportion of SPUA particles. The red dotted lines and orange dots indicate the frequency with which the SPUA particles are smaller than that size. After the grinding process, 90% of the SPUA modifier particles were below 122.5 µm and the maximum particle size was 74.5 µm. This proved that the low-temperature grinding technology has high processing efficiency. Finally, SPUA particles obtained by low-temperature grinding and processing were used as asphalt binder modifiers in this study, and selected quality of asphalt binder was 6%, 9% and 12% as the modifier content.



(a) Molecular structure of the urea bond



(b) Molecular structure of the carbamate

Figure 1. Molecular structure of the urea bond and carbamate.**Table 2.** Technical properties of SPUA.

Solid Content/%	Viscosity/cps	Tensile Strength/MPa	Elongation at Break/%
81–85	≤800	28	375

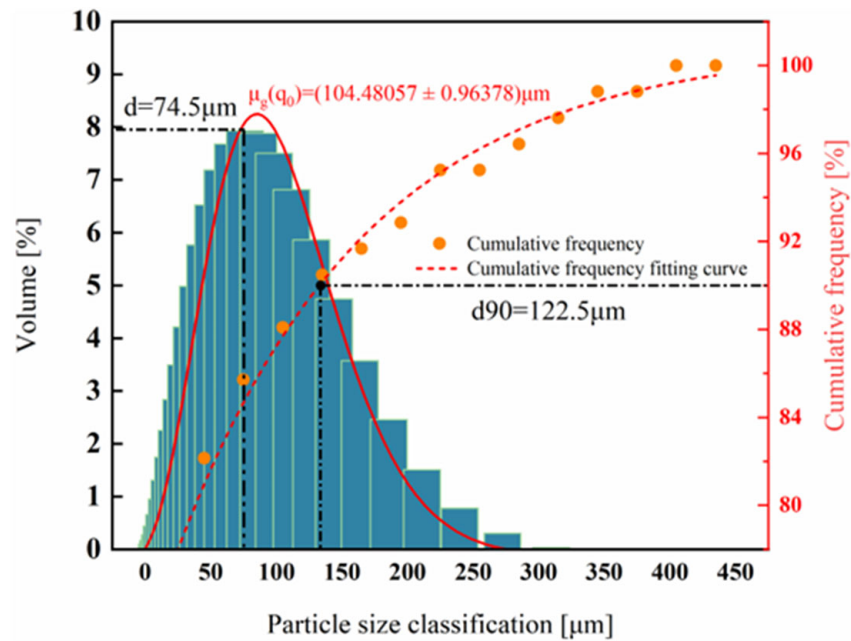


Figure 2. Particle size distribution of the SPUA modifier.

2.2. Test Method

The main research routes are shown in Figure 3. First, the optimum shearing time, rate and temperature of the SPMA were determined by an orthogonal test. On this basis, the high-temperature performance and fatigue performance of SPMA with different contents were studied. Among them, the high-temperature performance included the RV test, PG test and MSCR test. The fatigue performance tests included the LAS test and the TS test. Finally, applicability of various performance indexes to the SPMA was evaluated.

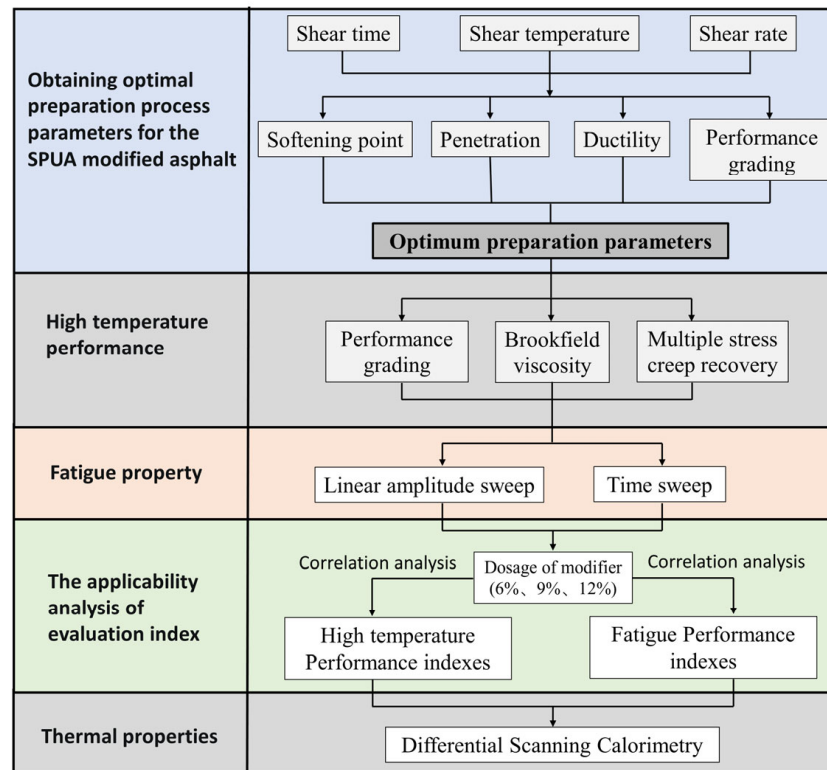


Figure 3. Research routes.

2.2.1. Orthogonal Experimental Design

Previous research results have indicated that shear time, rate and temperature are important factors affecting the cementing properties of modified asphalt [26–28]. Proper shear time and temperature are conducive to swelling of polymer modifiers in asphalt binders and promote interaction between asphalt binders and modifiers. The appropriate shear rate has a positive effect on the dispersion and uniformity of the modifier in the asphalt binder.

Therefore, in this study, the $L_9(3^4)$ orthogonal test table was made with shear time, rate and temperature as factors. However, the interaction between factors was not considered in this study, and the fourth column of the orthogonal test table was used as a blank column [28]. The content of SPUA in orthogonal test is 9%. This is because when the content of SPUA changes from 9% to 6% or 12%, only the content change is 3%, which reduces the influence of the content change on the test results.

In the early preparation, it was found that the base asphalt binder used in this study was sensitive to temperature: when the temperature was low (120 °C), the base asphalt binder could be completely melted, exhibiting good fluidity; when the temperature was close to 160 °C, there was an obvious smoke phenomenon of asphalt binder, accompanied by deterioration of ductility. This was caused by the high content of light components in the base asphalt binder used. Given this, to avoid excessive influence of process parameters on the original properties of base asphalt binder and to corporately characterize the real effect of SPUA modifier on the properties of base asphalt binder, the level of the orthogonal test was selected within a reasonable range in this study [29,30]. The specific process parameters and orthogonal test tables are listed in Tables 3 and 4, respectively.

Table 3. The factor and levels table of the orthogonal experiment.

Factors			
Levels	Shear time (A)	Shear rate (B)	Shear temperature (C)
	3000 rpm	10 min	120 °C
	4000 rpm	25 min	135 °C
	5000 rpm	40 min	150 °C

Table 4. Orthogonal test table.

Test Number	Shear Time (A)	Shear Rate (B)	Shear Temperature (C)	Test Program
1	120 °C	10 min	5000 rpm	A ₁ B ₁ C ₁
2	120 °C	25 min	6000 rpm	A ₁ B ₂ C ₂
3	120 °C	40 min	7000 rpm	A ₁ B ₃ C ₃
4	135 °C	10 min	6000 rpm	A ₂ B ₁ C ₂
5	135 °C	25 min	7000 rpm	A ₂ B ₂ C ₃
6	135 °C	40 min	5000 rpm	A ₂ B ₃ C ₂
7	150 °C	10 min	7000 rpm	A ₃ B ₁ C ₃
8	150 °C	25 min	5000 rpm	A ₃ B ₂ C ₁
9	150 °C	40 min	6000 rpm	A ₃ B ₃ C ₂

2.2.2. Modified Asphalt Binder Preparation Process

First, the base asphalt binder was put into the oven at 135 °C for 1.5 h until it was completely melted. The corresponding mass of SPUA was divided into three equal parts and added to the base asphalt binder in turn. To ensure the initial mixing of SPUA and the base asphalt binder, a glass rod should be used to stir manually for 1 min after each SPUA addition. Then, the asphalt binder was placed in an oil bath at the corresponding shear temperatures (120 °C, 135 °C and 150 °C) and held for 30 min. The asphalt binder was then prepared using a high-speed shear according to the process parameters determined in the orthogonal test table. The sheared asphalt binder was put into a 135 °C oven for 1 h to

provide conditions for the swelling of SPUA. Finally, the glass rod was used to slowly stir the finished asphalt binder to eliminate the tiny air bubbles. The modified asphalt binder preparation process is shown in Figure 4.

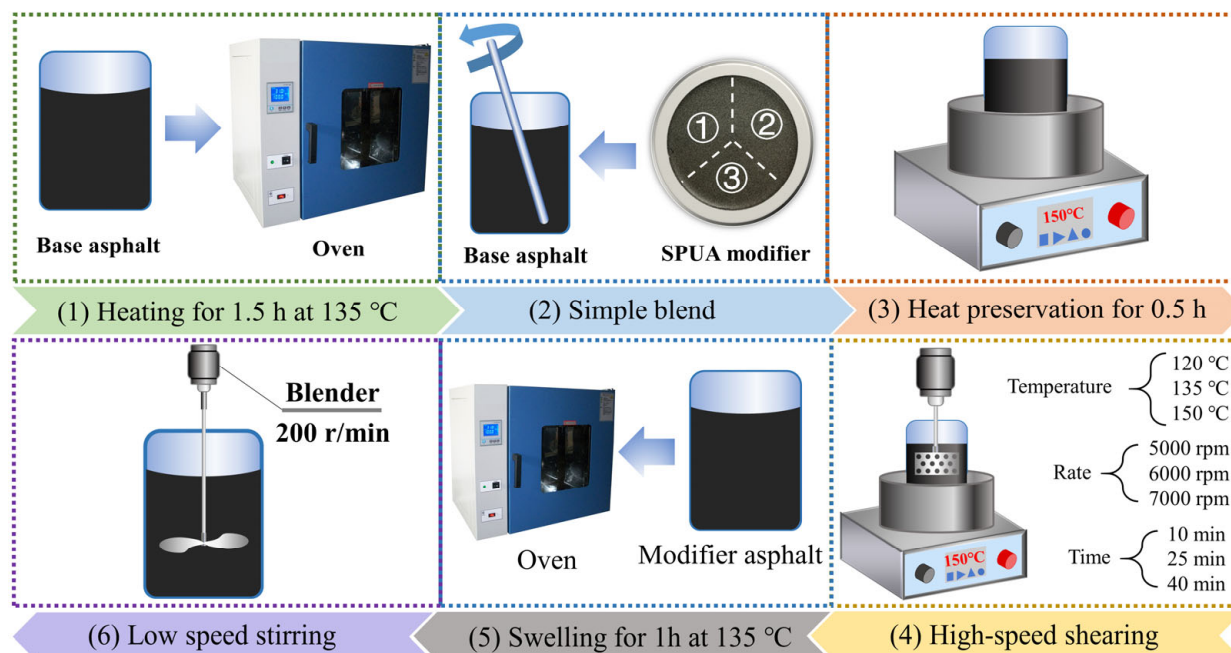


Figure 4. The modified asphalt preparation process.

2.2.3. Basic Performance Evaluation

The softening point, penetration (25 °C) and ductility (10 °C) of the modified asphalt were measured according to ASTM D113, ASTM D5 and ASTM D36, respectively. The testing instruments of softening point, penetration, and ductility were the WSY-025F asphalt softening point tester, WSY-026C automatic asphalt penetration tester, and LYY-10A asphalt elongation tester produced by Wuxi Petroleum Company of China.

2.2.4. High-Temperature Rheological Properties

a. Brookfield viscosity test

Brookfield viscosity was performed test according to ASTM D4402. The test temperatures were selected as 90 °C, 115 °C, 135 °C, 155 °C and 175 °C. Brookfield viscosity instrument was NDJ-1F produced by Changji Company in Shang-hai, China.

b. Performance grade test

In this study, the Smartpave102 dynamic shear rheometer from Anton Paar (Graz, Austria) was used. The performance grade (PG) test was performed according to ASTM D7643-10. The test was performed with a 25 mm diameter rotor, and the gap between parallel plates was controlled at 1 mm. The loading strain and frequency were 12% and 10 rad/s. The test temperature range was 46–76 °C, and the temperature rise interval was 6 °C.

c. Multiple stress creep recovery test

The multiple stress creep recovery (MSCR) test was performed according to ASTM-D7404-10a. The test temperature was chosen to be 64 °C. The rotor of the rheometer was 25 mm with a clearance control of 1 mm. First, the asphalt binder was loaded 20 times in a “load-recovery” cycle under a 0.1 kPa load. In this case, the first 10 cycles of loading were to equilibrate the specimens. Then, the asphalt binder was cyclically loaded 10 times under

a 3.2 kPa load. In each cycle of loading, the asphalt binder specimens were loaded for 1 s and unloaded for 9 s. The specific calculation equations are as follows:

$$R = \frac{\gamma_p - \gamma_{nr}}{\gamma_p - \gamma_0} \quad (1)$$

$$J_{nr} = \frac{\gamma_r - \gamma_0}{\tau} \quad (2)$$

$$J_{nr-diff} = \frac{[J_{nr}(3.2 \text{ kPa}) - J_{nr}(0 - 1 \text{ kPa})]}{J_{nr} 0.1 \text{ kPa}} \times 100\% \quad (3)$$

where γ_p was the peak strain within each cycle (%), γ_{nr} was the residual strain within each cycle (%) and γ_0 was the initial strain within each cycle (%); τ was the load (kPa).

2.2.5. Fatigue Performance

The fatigue test temperatures in this study were all 25 °C. The rotor diameter was chosen to be 8 mm and the clearance was controlled at 2 mm.

a. Linear amplitude sweep test

The linear amplitude sweep (LAS) test was conducted in accordance with AASHTO TP 101. The non-destructive characteristic value α of the asphalt binder was first determined by frequency scanning. The strain of the amplitude sweep increased linearly from 0% to 30% within 5 min. The calculation method is as follows:

First, the cumulative strength of the damage $D(t)$ was calculated.

$$D(t) \cong \sum_{i=1}^N \left[\pi \gamma_0^2 (C_{i-1} - C_i) \right]^{\frac{\alpha}{1+\alpha}} \cdot (t_i - t_{i-1})^{\frac{1}{1+\alpha}} \quad (4)$$

where C_i was the integrity parameter, calculated as $C(t) = \frac{|G^*(t)|}{|G^*|_{initial}}$, $|G^*|$ was complex shear modulus; γ_0^2 was the strain value (%) of the measured data points and t was the test time.

Then, $C(t)$ and $D(t)$ were fitted according to Equation (5) and the curve fitting coefficients C_1 and C_2 were obtained.

$$C(t) = C_0 - C_1(D)^{C_2} \quad (5)$$

where C_0 was the initial value of C , $C_0 = 1$; C_1 and C_2 were the damage fitting parameters.

D_f was then defined as the damage value of the asphalt material at the peak shear stress corresponding to the failure. the formula for D_f was given in Equation (6).

$$D_f = \left(\frac{C_0 - C \text{ at peak stress}}{C_1} \right)^{\frac{1}{C_2}} \quad (6)$$

Finally, the fatigue life N_f of the asphalt material was calculated by Equation (7).

$$N_f = A(\gamma_{max})^{-B} \quad (7)$$

where N_f was the fatigue life; A and B were parameters; γ_{max} was the maximum allowable strain, including 2.5% and 5%. Equations for A and B were shown in Equations (8) and (9).

$$A = \frac{f(D_f)^k}{k(\pi C_1 C_2)^\alpha} \quad (8)$$

$$B = 2\alpha \quad (9)$$

where f was the loading frequency (10 Hz); $k = 1 + (1 - C_2)\alpha$. C_1 and C_2 were damage curve fitting parameters.

b. Time sweeping test

The time sweeping (TS) was in strain control mode with a strain of 5%. This was determined from strain scans to ensure that the asphalt binders were in a linear viscoelastic range during the test. The *DER* is calculated as follows:

$$W_i = \int \delta(t) \frac{d\varepsilon(t)}{d(t)} dt = \pi \delta_i \varepsilon_i \sin(\delta_i) \quad (10)$$

$$W_c = \sum_{i=1}^n W_i \quad (11)$$

$$DER_i = \frac{\sum_{i=1}^n W_i}{W_n} = \frac{W_c}{W_n} \quad (12)$$

where W_i was the dissipation energy at the cycle i ; W_c was the cumulative dissipation energy; DER_i was the cumulative dissipation energy ratio during the cycle i ; $\sigma(t)$ was the stress, t was the time; $\varepsilon(t)$ was the strain; δ_i was the phase angle at the cycle i ; W_n was the dissipation energy at the cycle n .

2.2.6. Differential Scanning Calorimetry Test

DSC3 differential scanning calorimeter produced by Mettler Toledo, Greifensee, Switzerland, was adopted in this section. The samples were about 8–9 mg, and the samples were made of aluminum. The test temperature was -20 – 200 °C, and the heating rate was 10 °C/min.

3. Results and Discussion

3.1. Orthogonal Test Analysis

The results of orthogonal tests were often analyzed by the extreme difference analysis method and ANOVA, which were used to determine the optimal production conditions. Among them, the extreme difference analysis method can determine the degree of influence of the factor on the performance index based on the R-index of the factor. The ANOVA method can determine whether a factor is significant for a performance indicator based on the p -value. The results of the orthogonal test are shown in Figure 5.

3.1.1. Extreme Difference Analysis Method

The results of the extreme difference analysis for the failure temperature, softening point, penetration and ductility tests are listed in Tables 5–8, respectively. From the R in Tables 5–7, the optimal process parameters combination corresponding to failure temperature, softening point and pinning degree was $A_3B_3C_3$. The influence degree of the factors on the performance indexes in descending order were C (shear temperature) > A (shear time) > B (shear rate). This indicated that shear temperature was the most important factor affecting the failure temperature, softening point and penetration of the SPMA. Failure temperature and softening point were the indexes of high-temperature performance of asphalt binder [18]. The penetration represented the consistency of the asphalt, which indirectly reflected the high-temperature performance [31]. Therefore, this may be the reason why the three indicators had the same optimal process mix.

It was noteworthy that all the above three performance indexes reached their optimal values at level 3, which pinpointed that increasing the shear time, rate and temperature were all beneficial to improve the high-temperature performance and consistency of the SPMA. According to the available research results, this was mainly due to the following reasons: the increase in shear time, temperature and rate accelerated the swelling of the modifier, promoted the combination of the modifier with the asphalt mastic and improved the dispersion of the modified asphalt [26]. Second, the increased shear time, temperature and rate promoted volatilization and transformation of light components within the asphalt, accelerating the oxidation and aging of the asphalt components [32].

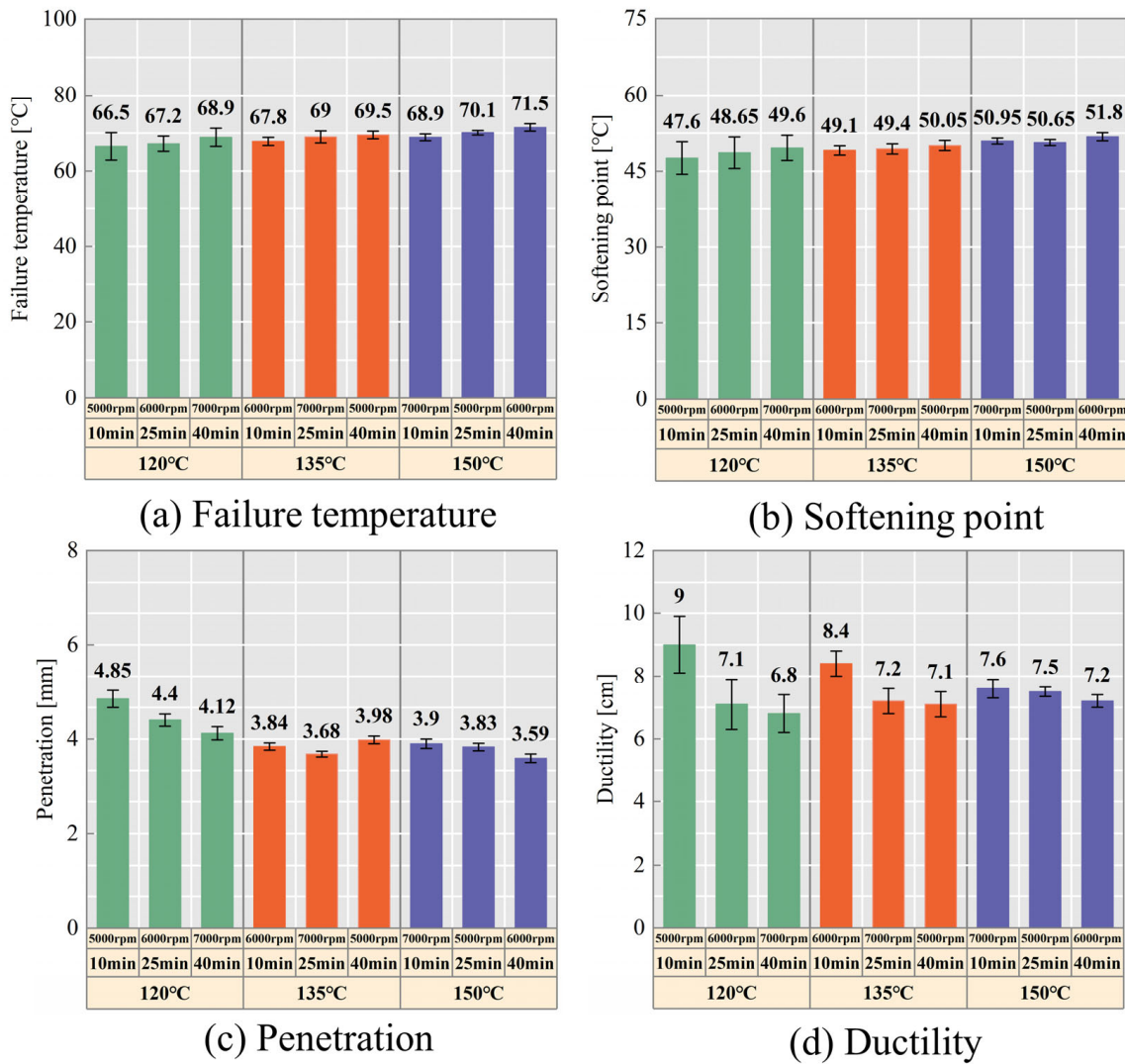


Figure 5. Orthogonal experimental results.

Table 5. Failure temperature range analysis results.

Test Number	Shear Time	Shear Rate	Shear Temperature	Blank Group	Failure Temperature
1	1	1	1	1	66.5
2	2	2	1	2	67.2
3	3	3	1	3	68.9
4	1	2	2	3	67.8
5	2	3	2	1	69
6	3	1	2	2	69.5
7	1	3	3	2	68.9
8	2	1	3	3	70.1
9	3	2	3	1	71.5
K1	203.20	206.10	202.60	207.00	-
K2	206.30	206.50	206.30	205.60	-
K3	209.90	206.80	210.50	206.80	-
k1	67.73	68.70	67.53	69.00	-
k2	68.77	68.83	68.77	68.53	-
k3	69.97	68.93	70.17	68.93	-
R	2.23	0.23	2.63	0.47	-

$R_C > R_A > R_B$, optimal process: $A_3B_3C_3$

Table 6. Softening point range analysis results.

Test Number	Shear Time	Shear Rate	Shear Temperature	Blank Group	Softening Point
1	1	1	1	1	47.6
2	2	2	1	2	48.65
3	3	3	1	3	49.6
4	1	2	2	3	49.1
5	2	3	2	1	49.4
6	3	1	2	2	50.05
7	1	3	3	2	50.95
8	2	1	3	3	50.65
9	3	2	3	1	51.8
K1	147.65	148.30	145.85	148.80	-
K2	148.70	149.55	148.55	149.65	-
K3	151.45	149.95	153.40	149.35	-
k1	49.22	49.43	48.62	49.60	-
k2	49.57	49.85	49.52	49.88	-
k3	50.48	49.98	51.13	49.78	-
R	1.27	0.55	2.52	0.28	-

$R_C > R_A > R_B$, optimal process: $A_3B_3C_3$

Table 7. Penetration range analysis results.

Test Number	Shear Time	Shear Rate	Shear Temperature	Blank Group	Penetration
1	1	1	1	1	4.9
2	2	2	1	2	4.4
3	3	3	1	3	4.1
4	1	2	2	3	3.8
5	2	3	2	1	3.7
6	3	1	2	2	4.0
7	1	3	3	2	3.9
8	2	1	3	3	3.8
9	3	2	3	1	3.6
K1	12.59	12.66	13.37	12.12	-
K2	11.91	11.83	11.50	12.28	-
K3	11.69	11.70	11.32	11.79	-
k1	4.20	4.22	4.46	4.04	-
k2	3.97	3.94	3.83	4.09	-
k3	3.90	3.90	3.77	3.93	-
R	0.30	0.32	0.68	0.16	-

$R_C > R_B > R_A$, optimal process: $A_3B_3C_3$

From Table 8, the factors affecting the index of ductility were A (shear time) > B (shear rate) > C (shear temperature) in order, and the optimal preparation parameters were $A_1B_1C_1$. It can be found that the ductility decreased with an increase in the three factors. The reason for this was mainly due to the transformation of the components and the aging of the asphalt to improve the stiffness of the asphalt binder.

The extreme difference analysis method can reflect the influence of different factors on performance, while it was still unclear whether the influence of different levels on the performance index was significant. Therefore, the following will combine the results of the ANOVA and further optimize the preparation parameters in terms of energy consumption and preparation efficiency.

Table 8. Ductility range analysis results.

Test Number	Shear Time	Shear Rate	Shear Temperature	Blank Group	Ductility
1	1	1	1	1	9.0
2	2	2	1	2	7.1
3	3	3	1	3	6.8
4	1	2	2	3	8.4
5	2	3	2	1	7.2
6	3	1	2	2	7.1
7	1	3	3	2	7.6
8	2	1	3	3	7.5
9	3	2	3	1	7.2
K1	25.00	23.60	22.90	23.40	-
K2	21.80	22.70	22.70	21.80	-
K3	21.10	21.60	22.30	22.70	-
k1	8.33	7.87	7.63	7.80	-
k2	7.27	7.57	7.57	7.27	-
k3	7.03	7.20	7.43	7.57	-
R	1.30	0.67	0.20	0.53	-

$R_A > R_B > R_C$, optimal process: $A_1B_1C_1$

3.1.2. Analysis of Variance

From Tables 9–12, shear temperature had a significant effect on the failure temperature, softening point and penetration. Shear time had a significant effect on the failure temperature and softening point, and the shear rate had no significant effect on any of the four indices. Therefore, the shear rate can be reduced appropriately.

Table 9. Failure temperature variance analysis results.

Test Number	Shear Time	Shear Rate	Shear Temperature	Blank Group
Sj	7.50	0.08	10.42	0.38
DOF	2.00	2.00	2.00	2.00
MSE	3.75	0.04	5.21	0.19
F	19.61	0.22	27.25	1.00
P	0.05	0.82	0.04	0.50
Sig	√	×	√	

Note: √ indicated that the selected factors had a significant impact on the index and × indicated that the selected factors had no significant effect on the index.

Table 10. Softening point variance results.

Test Number	Shear Time	Shear Rate	Shear Temperature	Blank Group
Sj	2.57	0.49	9.76	0.12
DOF	2.00	2.00	2.00	2.00
MSE	1.28	0.25	4.88	0.06
F	20.72	3.99	78.76	1.00
P	0.05	0.20	0.01	0.50
Sig	√	×	√	-

Note: √ indicated that the selected factors had a significant impact on the index and × indicated that the selected factors had no significant effect on the index.

Table 11. Penetration variance results.

Test Number	Shear Time	Shear Rate	Shear Temperature	Blank Group
Sj	0.15	0.18	0.86	0.04
DOF	2.00	2.00	2.00	2.00
MSE	0.07	0.09	0.43	0.02
F	3.53	4.34	20.64	1.00
P	0.22	0.19	0.05	0.50
Sig	×	×	√	-

Note: √ indicated that the selected factors had a significant impact on the index and × indicated that the selected factors had no significant effect on the index.

Table 12. Ductility variance results.

Test Number	Shear Time	Shear Rate	Shear Temperature	Blank Group
Sj	2.88	0.67	0.06	0.43
DOF	2.00	2.00	2.00	2.00
MSE	1.44	0.33	0.03	0.21
F	6.72	1.56	0.15	1.00
P	0.13	0.39	0.87	0.50
Sig	×	×	×	-

Note: × indicated that the selected factors had no significant effect on the index.

In addition, by comparing the k values in the results of the extreme difference analysis, it can be found that, for the failure temperature, softening point and penetration, the difference between k3 at the optimal level and k2 was not significant. For the ductility, the difference between k1 at the optimal level and k2 was not significant. Therefore, considering the high- and low-temperature performance and energy consumption, A₃B₂C₃ (shear time, rate and temperature of 40 min, 6000 rpm and 150 °C, respectively) was selected as the best process parameter for preparing the SPMA.

3.2. High-Temperature Rheological Properties

3.2.1. Brookfield Viscosity

(1) Apparent viscosity

The SPMA with different dosages were prepared using optimal process parameters. Figure 6 manifested the viscosity–temperature curves of the asphalt binder, showing the effect of modifier and temperature on the apparent viscosity of the asphalt binder. Enhancement in temperature intensified the thermal movement of molecules, manifested as a gradual decrease in the viscosity–temperature curve of asphalt binder, easier to overcome the frictional resistance between molecules and produce flow deformation [33]. To ensure that the asphalt binder had good constructability, the specification requires the apparent viscosity of less than 3 Pa·s at 135 °C. Figure 5 displayed that the viscosity of the different asphalt binders was already less than 3 Pa·s at 115 °C. This demonstrated that the modified asphalt can be applied at lower temperatures, which reduced energy consumption and waste gas emissions [34].

In addition, the modifier enhanced the viscosity of the asphalt binder. With the boost in dosage, the improvement in viscosity was more obvious. For example, at 135 °C, the viscosity of 6%, 9% and 12% modified asphalt binders increased by 10.8%, 28.5% and 52.2%, respectively, compared to the base asphalt binder. This revealed that addition of modifiers impeded the flow of asphalt binder and had a positive effect on the high-temperature performance [35,36].

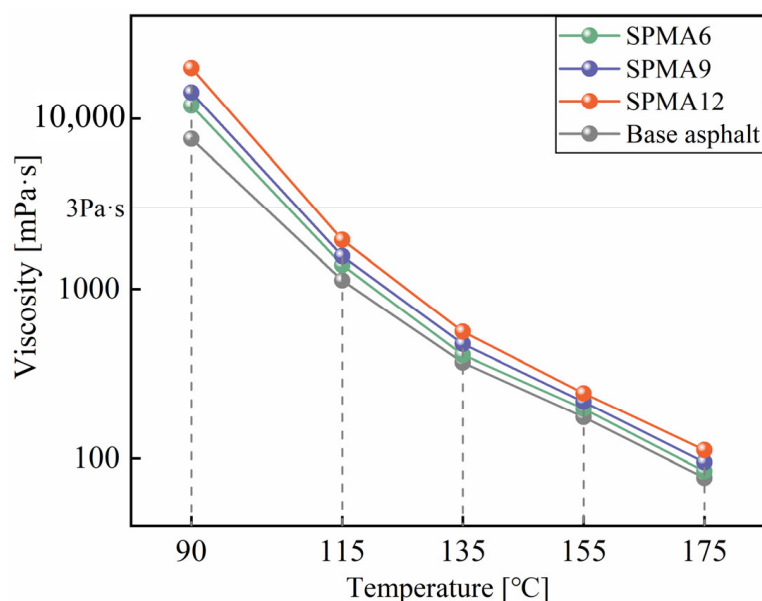


Figure 6. Apparent viscosity of asphalt binders.

(2) Activation energy

In addition, the temperature sensitivity of the asphalt binder was calculated by Arrhenius Equation (13) [37]. The specific calculation formula is as follows:

$$\eta = A \cdot e^{\frac{E_a}{RT}} \quad (13)$$

where η was the apparent viscosity of asphalt binder, A was the fitting parameter, E_a (kJ/mol) was the activation energy of asphalt mastic, R was the gas constant, $R = 8.314 \text{ J}/(\text{mol}\cdot\text{K})$ and K was the absolute temperature.

After processing, the Arrhenius Equation (13) can be expressed by Equation (14).

$$\ln \eta = \ln A + \frac{E_a}{R} \times \frac{1}{T} \quad (14)$$

The activation energy of the asphalt binders is exhibited in Figure 7. The specific calculation results are shown in Table 13. The R^2 was greater than 0.97, which expressed a good fitting result. With the addition of 6%, 9% and 12% modifiers, the activation energy of the asphalt binders grew by 7.4%, 8.8% and 13.0% compared to the base asphalt binder. As a result, the asphalt binder required more external energy when it produced flow deformation. This implied that mounting the modifier content improved the temperature sensitivity of the asphalt binder [34,38]. It may be related to the following reasons: first, the polymer modifier will absorb the light component of the asphalt binder in the process of swelling, which indirectly enhanced the content of heavy components in the asphalt system [39]. Second, when the polymer modifier was mixed with the asphalt binder, the stiffness and internal friction resistance will be increased, which will hinder the flow of the asphalt binder [37,40]. Under the synergistic action of the above two reasons, the activation energy of asphalt binder improved with the addition of modifier content.

Table 13. The fitting result of activation energy.

Asphalt Type	E_a (Slope, kJ/mol)	A (Intercept)	R^2
Base asphalt	21.5	−7.4	0.98
SPMA6	23.1	−8.1	0.98
SPMA9	23.4	−8.2	0.97
SPMA12	24.3	−8.5	0.97

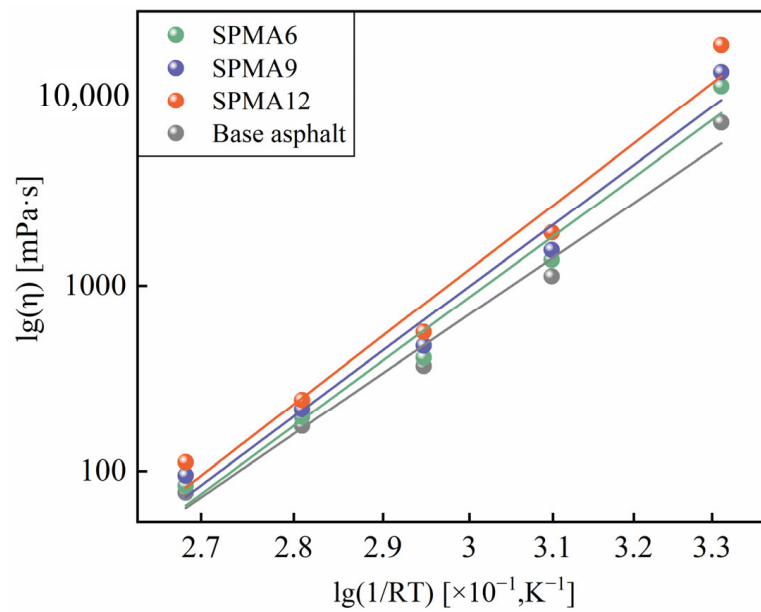


Figure 7. Activation energy of asphalt binders.

3.2.2. PG Test

(1) Rutting factor

Figure 8a shows the $G^*/\sin\delta$ of asphalt binder as a function of temperature. It was obvious that the enhancement in temperature reduced the $G^*/\sin\delta$, revealing a negative effect on the deformation resistance at high temperatures. Meanwhile, in agreement with the prediction, the addition of modifiers improved the $G^*/\sin\delta$. Moreover, the high-temperature failure temperature of the asphalt binder was calculated according to the specification. In the specification, the high-temperature failure temperature was defined as the temperature at the $G^*/\sin\delta$ of 1 kPa, and the calculation results are shown in Figure 8b. It can be found that the failure temperature gained by 5.89 °C, 6.23 °C and 9.8 °C respectively with the addition of modifier dosage. This meant that the modifier improved the high-temperature deformation resistance of the asphalt binders, which was equivalent to expanding the ambient temperature range that the asphalt binder can withstand during the service life. This was due to the absorption of light components and polymer network formation by the modifier [17].

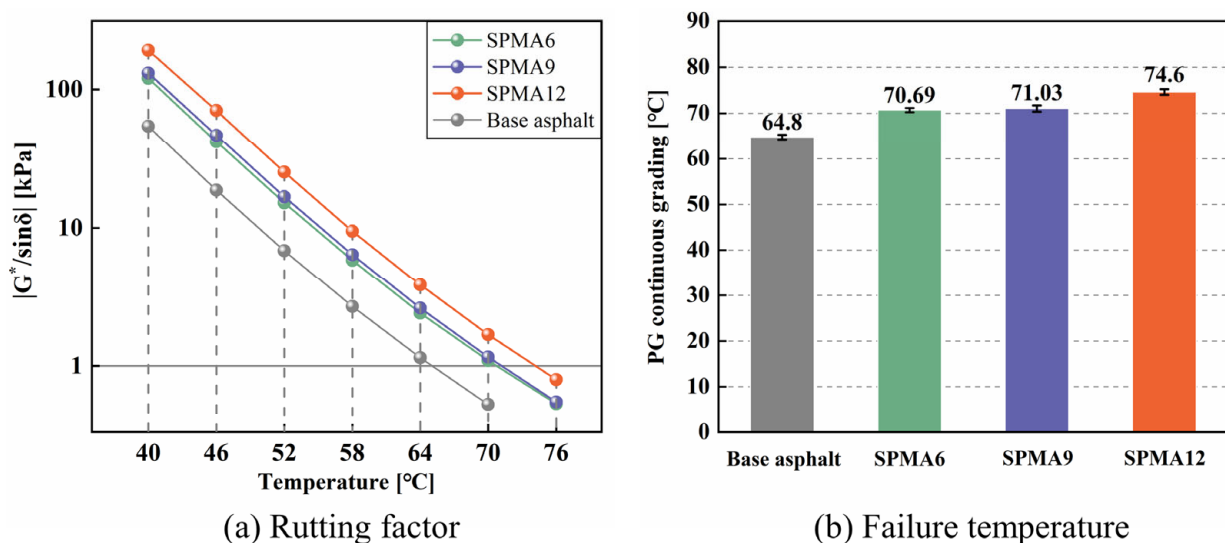


Figure 8. Rutting factor of asphalt binders.

It was noteworthy that the failure temperatures of the modified asphalt with 6%, 9% and 12% dosage were increased by 9.1%, 9.6% and 15.1% relative to the base asphalt binder. It can be found that the $G^*/\sin\delta$ of the modified asphalt binder did not produce a significant increase when increasing from 6% to 9%, and the same phenomenon was reflected in the $G^*/\sin\delta$ curve. This may be related to the sensitivity of the test method to the viscoelastic properties of the asphalt binder.

In order to investigate the applicability of the $G^*/\sin\delta$ of the PG test to the characterization of the high-temperature properties, two improved rutting factors: $G^*/(\sin\delta)^9$ and $G^*/[1 - 1/(\tan\delta\sin\delta)]$ were also used in this paper to analyze the test results. The specific results are manifested in Figure 9. The results demonstrated that the two improved rutting factors can obviously reflect the performance difference between modified asphalt and base asphalt but still cannot effectively reflect the high-temperature performance of modified asphalt at 6% and 9% dosage.

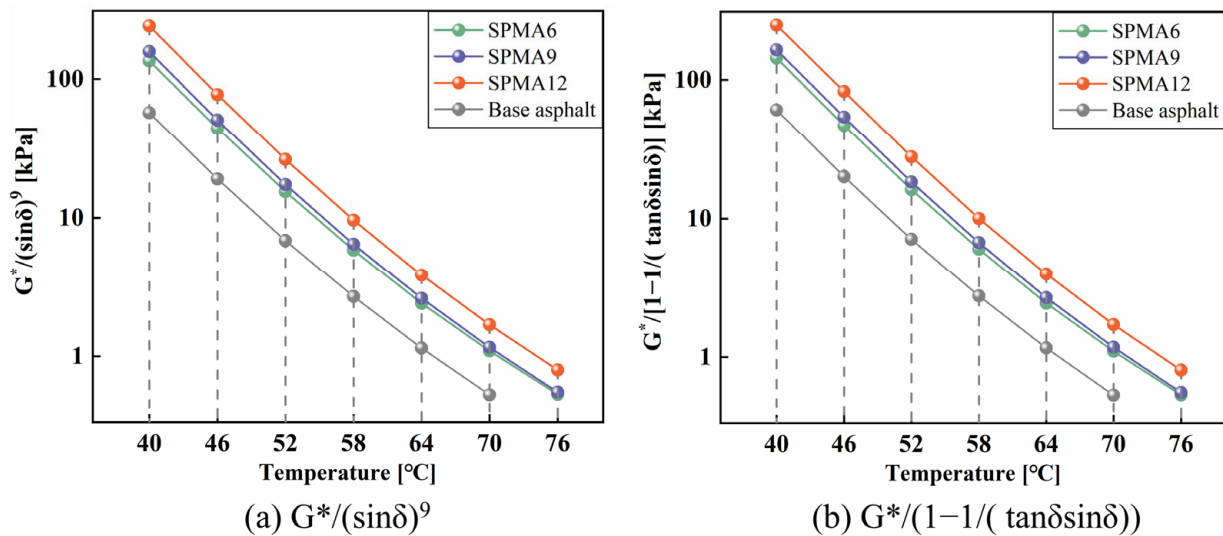


Figure 9. Improved rutting factor.

(2) Phase angle

Figure 10 reveals the results of the phase angle for the PG test. As the temperature increased, the phase angle showed a gradual increase. It meant that the improvement in temperature caused the asphalt binder to gradually lose its elastic properties and transformed into a fully cohesive material. Compared with the base asphalt, the SPMA can effectively reduce the phase angle, and the reduction was enhanced with an increase in the dosage. For example, at 40 °C, the phase angles of the modified asphalt with 6%, 9% and 12% dosage decreased by 3.5°, 6.1° and 7.6° compared to the base asphalt. This signaled that the modifier played a positive role in the elastic recovery performance of the asphalt binder, enabling it to recover quickly after deformation. This was because the modifier changes the colloidal structure of the asphalt binder and improves the internal elasticity of the components.

(3) Temperature susceptibility

In addition, The $G^*/\sin\delta$ -T curves in logarithmic coordinates were used to characterize the temperature sensitivity:

$$\ln|G^*| = A\ln T + B \tag{15}$$

Parameter A was the temperature sensitivity index; its larger absolute value represented higher temperature sensitivity of asphalt binder. The fitting results are shown in Figure 11 and Table 14. The temperature sensitivity of asphalt binder was boosted with the addition of modifier dosage in the range of 40–70 °C, which signified that, the greater the dosage of SPMA, the more obvious the magnitude of high-temperature performance

deterioration in the process of temperature rise. This was because of the incompatibility between the modifier and the asphalt binder, and the strength of the bonding interface was susceptible to weakening due to temperature effects, which reduced the contribution of the bonding properties to the strength of the asphalt binder. The higher the modifier dose, the more the bonding interface inside the asphalt binder and the greater the strength weakening at elevated temperatures, which explained the increase in temperature sensitivity of asphalt binder with additional modifier dosage from 40–70 °C.

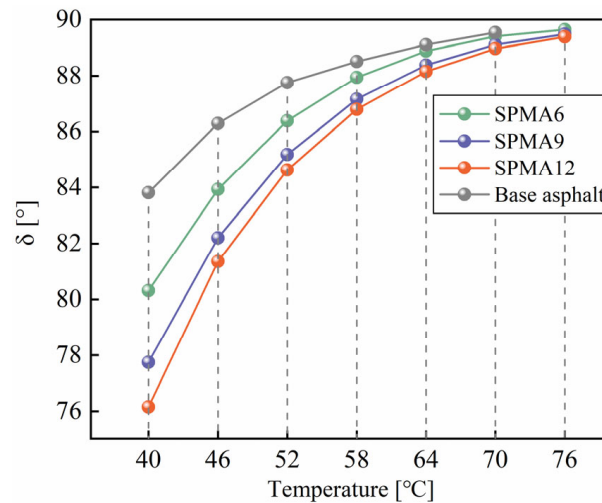


Figure 10. The phase angle of asphalt binders.

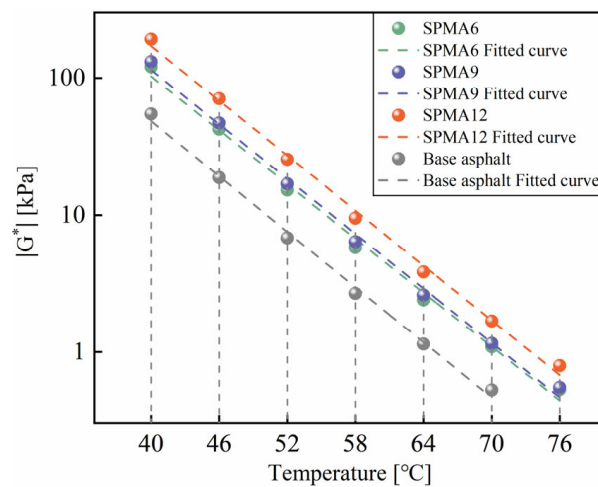


Figure 11. Temperature sensibility.

Table 14. The fitting result of temperature sensibility.

Asphalt Type	A (Slope)	B (Intercept)	R ²
Base asphalt	8.32	18.10	0.99
SPMA6	8.53	18.79	0.99
SPMA9	8.61	18.97	0.99
SPMA12	8.64	19.20	0.99

Notably, this was not consistent with the temperature-sensitive results for Brookfield viscosity. This was probably due to the different contributions of internal friction resistance, bonding properties, etc., to temperature sensitivity in different temperature ranges. In the range of 40–70 °C, the internal friction resistance and the bonding properties of the modifier and the asphalt binder together played a positive role in the temperature sensitivity.

However, as the temperature enhanced to within the Brookfield viscosity test temperature range, the asphalt binder took on a liquid state. At this time, the bonding effect between the asphalt binder and the modifier disappears and the internal friction resistance into the impact for the main factors of temperature sensitivity. The internal friction resistance was positively correlated with the modifier dosage, so the temperature sensitivity of the asphalt binder improves with increasing admixture at the Brookfield viscosity test temperature.

3.2.3. MSCR Test

In response to the inability of the PG test to effectively distinguish the difference in high-temperature performance between 6% and 9% modified asphalt binders, this study used the MSCR test for asphalt binders. Figure 12 shows the stress–strain relationship of the asphalt binder during the loading process. As can be seen from the figure, the strain of asphalt binders in the cyclic loading process constantly made the accumulation, resulting in irrecoverable deformation. Compared with 0.1 kPa load, the asphalt binder under 3.2 kPa load had higher cumulative deformation. This explained the greater susceptibility to rutting on asphalt roads with high traffic volumes and overloaded vehicles [18].

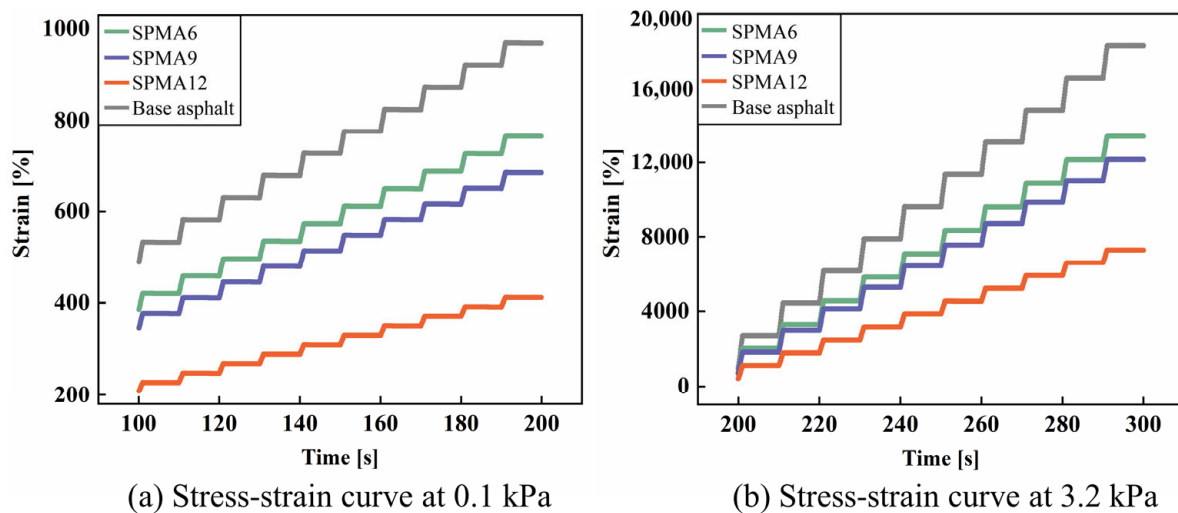


Figure 12. MSCR test results of asphalt binders.

Meanwhile, the strain value of asphalt binder decreased with an increase in modifier dosage. This indicated that the addition of the modifier reduced the deformation of asphalt binders, playing a positive effect on the anti-deformation performance. It had a positive effect on the deformation resistance, and the high-temperature performance can be further improved by increasing the modifier content.

Interestingly, at a load of 0.1 kPa, there was a significant difference between the 6% and 9% dosage of modified asphalt, implying a higher sensitivity of the MSCR test to the viscoelastic properties of the asphalt binders.

In addition, two other viscoelastic indices of asphalt binders can be obtained from the MSCR test: the recovery rate (R) and the irrecoverable creep flexibility (J_{nr}), where the R reflects the deformation recovery performance of the asphalt binder after unloading and J_{nr} reflects the level of permanent deformation of the asphalt binder under the load. As shown in Figure 13, the R of the base asphalt was only 0.02 at 0.1 kPa load, which almost completely lost the elastic recovery performance, and, after adding the modifier, the R of the asphalt binder improved significantly and gradually enhanced with an increase in modifier dosage. The R of SPMA improved by 0.85, 1.59 and 1.72 over the base asphalt binder with the addition of 6%, 9% and 12% doping modifiers, respectively. At 3.2 kPa load, with an increase in modifier dosage, the trend of R of asphalt binder was the same as that at 0.1 kPa load. The R of asphalt binders increased by 0.048, 0.058 and 0.148 at 6%, 9% and 12% modifier dosage, respectively. This illustrated that increasing the amount of

modifier was conducive to improvement in elastic recovery properties of asphalt binder. This was because the modifier improved the elastic component of the asphalt binders.

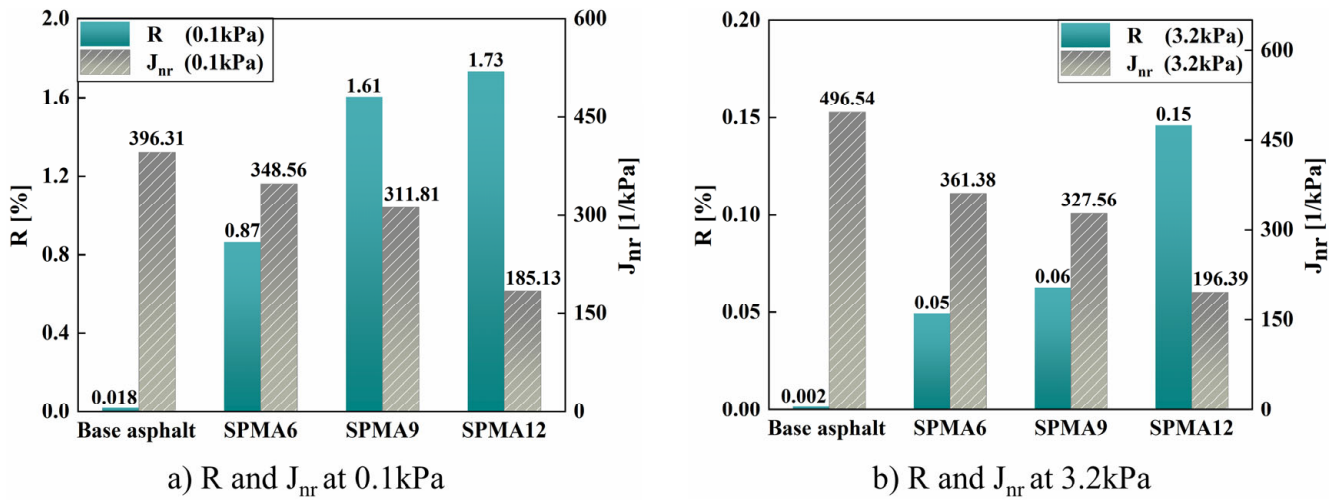


Figure 13. Calculating values of R and J_{nr} .

From Figure 13, the J_{nr} of asphalt binder decreases with the addition of modifier. At 0.1 kPa load, J_{nr} of asphalt binders with 6%, 9% and 12% modifier content was reduced by 12.5%, 2.3% and 53.3% compared with base asphalt binder, respectively. At 3.2 kPa load, J_{nr} of asphalt binders with 6%, 9% and 12% modifier content decreased by 27.2%, 34.0% and 60.4% compared with that of base asphalt binder, respectively. This meant that the modified asphalt with larger dosage had higher deformation resistance.

In addition, $J_{nr-diff}$ was used to characterize the stress sensitivity of the asphalt binder in the MSCR test. Figure 14 demonstrates the relationship between $J_{nr-diff}$ values and modifier dosage. As can be seen from the figure, the addition of the modifier reduced the stress sensitivity of the base asphalt binder. However, the stress sensitivity of the modified asphalt gradually increased with an increase in the modifier. It should be noted that, although the modified asphalt binders with high admixture were more sensitive to stress, this did not mean that the high admixture modifier was detrimental to the high-temperature performance of the asphalt binders. This was because the index only reflected the sensitivity of the asphalt binder to the applied stress.

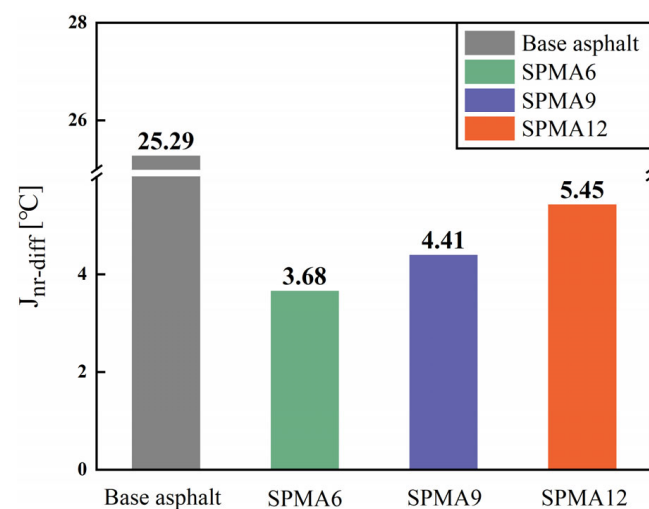


Figure 14. Calculating values of $J_{nr-diff}$.

3.3. Fatigue Performance Characterization

3.3.1. Fatigue Performance Analysis Based on LAS Test

Figure 15 describes the stress–strain curves of the asphalt binder in the LAS test. With an increase in strain, the stress rose rapidly at first and then decreased rapidly after reaching the maximum value. The relevant literature referred to the strain corresponding to the peak stress in the curve as the yield strain and defines it as the breaking point of the asphalt binder [41]. The yield strains of the base asphalt binder and the modified asphalt with different admixtures were 7.6%, 7.99%, 8.28% and 9.26%, respectively. This indicated that the modifier advanced the hardness of the asphalt binder [42].

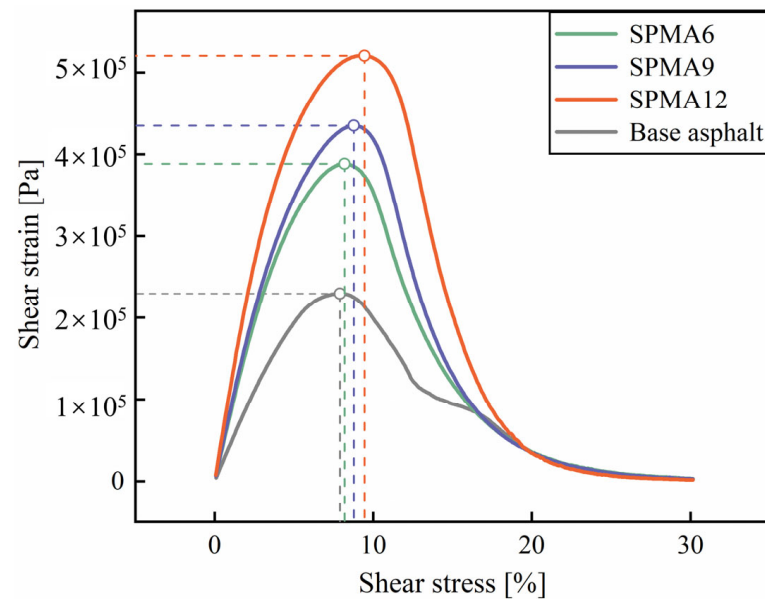


Figure 15. Stress–strain curve of asphalt binders.

Figure 16 displays the fatigue damage characteristic curves obtained by fitting the S-VECD model. The vertical coordinate of S-VECD was the integrity parameter (C) and the horizontal coordinate was the cumulative damage intensity. The high C signified that the asphalt mastic had excellent fatigue resistance [43]. It can be found that, when the damage intensity was small, the integrity parameters of different asphalt binders were the same. As the damage intensity gradually escalated, the integrity of the base asphalt decreased rapidly and the difference with the SPMA gradually became distinct. This suggested that both the base asphalt binder and the modified asphalt binder had essentially the same fatigue resistance in the early stages of loading. However, the fatigue resistance of the base asphalt binder decayed rapidly as the damage intensity gradually grew, demonstrating a higher strain sensitivity of the base asphalt binder.

To quantitatively analyze the effect of modifiers on the fatigue resistance of asphalt binders, the fatigue performance parameters A and B and the fatigue life of asphalt binders were calculated. Parameter A represented the integrity of the asphalt binder, and, the larger parameter A , the better the fatigue resistance of the asphalt binder. Parameter B represented the strain sensitivity of the asphalt binder in the fatigue test; the larger parameter B , the stronger the strain sensitivity of the asphalt binder [44]. As shown in Figure 17a, the integrity of the asphalt binder boosted with an increase in modifier dosage: 6%, 9% and 12% modifier dosage of asphalt binder increased the parameter A by 99.1%, 135.3% and 539.6%, respectively, compared to the base asphalt binder, while the B parameter illustrated that the modifier was detrimental to the stress sensitivity of the asphalt binder under cyclic loading. This may predict a more substantial decay in the fatigue life of the SPMA with enhancing strain.

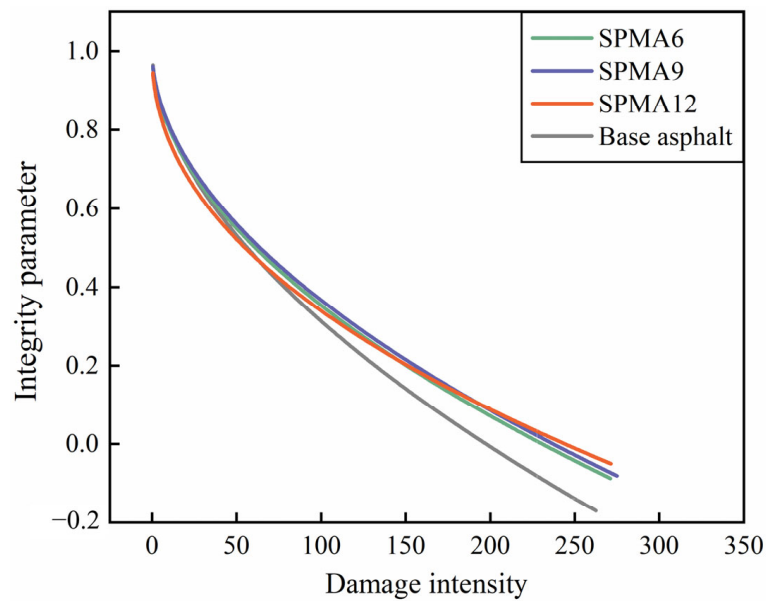


Figure 16. C–D curve of asphalt binders.

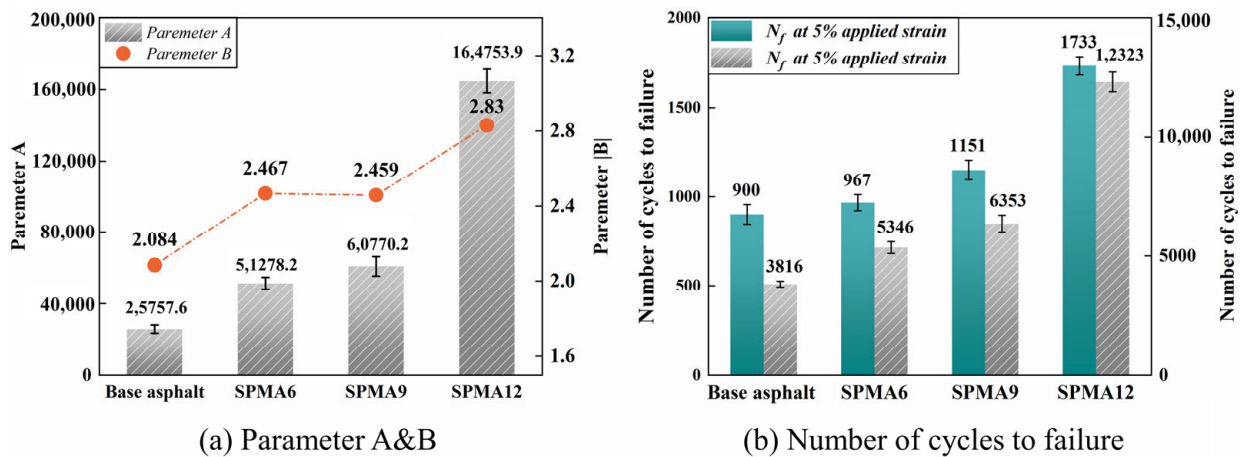


Figure 17. LAS test result of asphalt binders.

The fatigue life of the asphalt binder is shown in Figure 17b. When the strain was 2.5%, the fatigue life enhanced by 40.1%, 66.5% and 223.9%, respectively, with an increase in modifier content. When the strain is 5%, the fatigue life improved by 7.4%, 27.8% and 92.6%, respectively, with the increase in modifier content. This indicated that increasing the modifier content can significantly improve the fatigue properties of asphalt binder [45,46].

It can also be noted that, compared to the fatigue life at 2.5% applied strain, the fatigue life of the base asphalt binder and modified asphalt binder at 5% applied strain was reduced by 76.4%, 81.9%, 81.8% and 85.9%, respectively. This meant that the fatigue life of the modified asphalt binders was more sensitive to stress, and this sensitivity was more pronounced in the high admixture of the modified asphalt binder, which was consistent with the results predicted by parameter B. Similarly, an increase in sensitivity did not imply an improvement in fatigue life or decay. In conclusion, the fatigue life of asphalt binders can be effectively improved by increasing the content of modifiers.

3.3.2. Fatigue Performance Analysis Based on Time Scanning Test

Figure 18 displays the relationship between loading times and normalized modulus ($|G^*|/|G^*|_{initial}$) of the asphalt binder. The $|G^*|/|G^*|_{initial}$ of the asphalt binder gradually decreased as the number of loadings increased. This was due to the accumulation

of fatigue damage in the asphalt binder during cyclic loading, which caused its integrity to be destroyed and the modulus to decay rapidly [46]. The fatigue life N_{p50} of the base asphalt binder and modified asphalt binders were 1302, 1398, 1500 and 2202, respectively. Compared to the base asphalt binder, the N_{p50} of the modified asphalt binder with 6%, 9% and 12% dosage increased by 7.3%, 15.2% and 69.1%, respectively. This was as expected; the modifier enhanced the $|G^*|/|G^*|_{\text{initial}}$ of the asphalt binders and improved the fatigue performance. This was consistent with the LAS test results. The difference was that the $|G^*|/|G^*|_{\text{initial}}$ curves of the modified asphalt binder at 6% and 9% admixture are similar. This may be related to the loading methods of the TS test and LAS tests. A 0% to 30% strain, amplitude sweep was used in the LAS test to accelerate the fatigue damage, where some of the strains exceeded the linear viscoelastic range of the asphalt binders. In contrast, the TS test used 5% of the strain in the linear viscoelastic energy range. This may be the reason why the LAS test was more sensitive to viscoelastic energy and can effectively distinguish the fatigue performance of different asphalt binders.

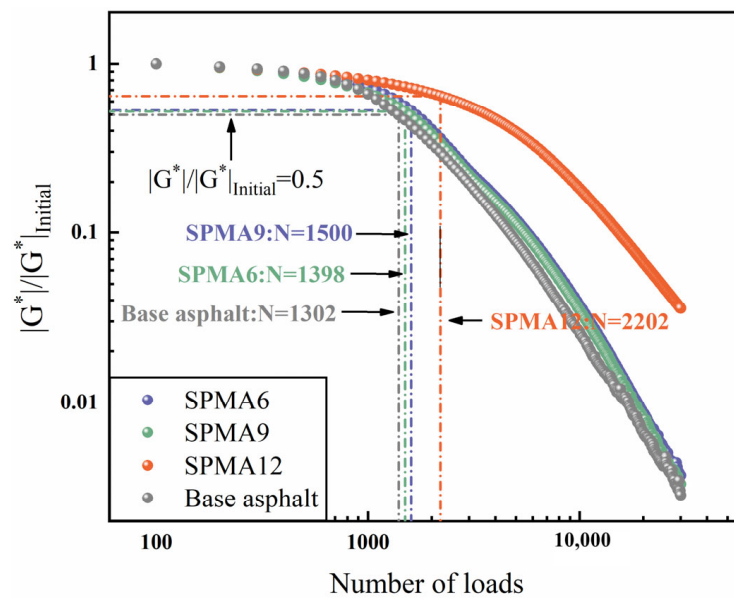


Figure 18. Normalized modulus curve of asphalt binders.

Meanwhile, the fatigue performance of the asphalt binder was analyzed from the perspective of energy dissipation. Figure 19 demonstrates the DER of asphalt binders versus the number of cyclic loading. At the early stage of the experiment, DER and N followed the lossless state curve with a slope of 1. As fatigue damage gradually accumulates, the DER gradually deviated from the lossless state curve. The number of loads corresponding to a 20% deviation of the DER- N curve from the nondestructive state curve was used as the fatigue life N_{p20} of the asphalt binder [17,25]. As shown in Figure 19, the modifiers had a positive effect on the fatigue life of the asphalt binder. The fatigue life N_{p20} of the base and modified asphalt binder were 601, 702, 799 and 1379, respectively. Compared to the base asphalt binder, the N_{p50} of the modified asphalt binder with 6%, 9% and 12% dosage increased by 16.8%, 32.9% and 129.5%, respectively. However, the DER- N curves of the modified asphalt binders at 6% and 9% admixture were similar.

It is worth noting that there was a significant difference between the fatigue life N_f obtained using the LAS test, N_{p50} obtained using the normalized modulus calculation and N_{p20} obtained using the dissipative energy calculation. This was because the selection of applied loads, frequencies and fatigue failure determination criteria in the TS test was artificially determined and highly empirical [25]. The fatigue life of the same asphalt binder can range from a few thousand to tens of thousands depending on the fatigue failure judgment criteria of the TS test. In contrast, the fatigue failure of asphalt binders should be a material's characteristic and should have obvious material dependence. Therefore,

from the sensitivity of the test to the asphalt binder and the accuracy and completeness of the evaluation system, the LAS test was more suitable as a test method for the fatigue performance of asphalt binders.

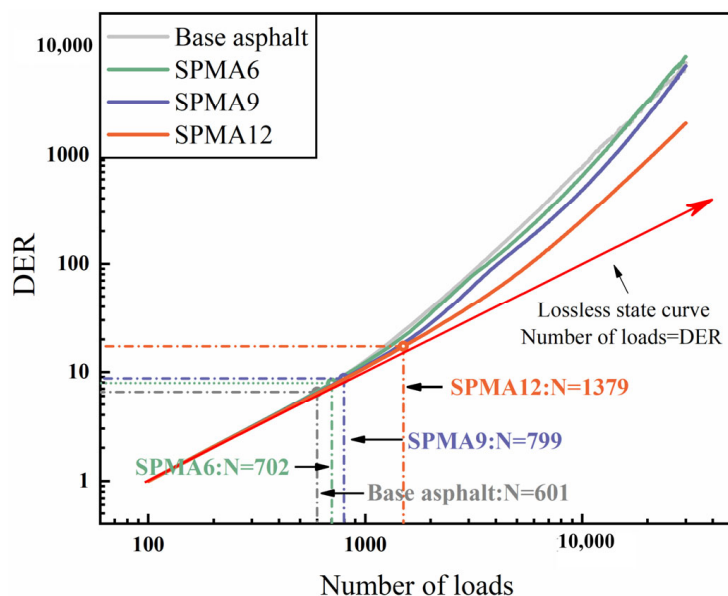


Figure 19. DER curve of asphalt binders.

3.4. Applicability of High-Temperature and Fatigue Indicators to the Performance Evaluation of Asphalt Binders

In summary, the SPUA had an excellent performance on asphalt binders for both high-temperature performance and fatigue performance improvement. However, it can be seen from Figures 20 and 21 that some of the tests were unable to effectively differentiate the viscoelastic properties of the modified asphalt binders in some of the admixture ranges (e.g., 6% and 9%), and this will be an obstacle to application and promotion of SPUA modifiers in practical engineering. Therefore, it was necessary to investigate the applicability of different tests and their corresponding metrics.

In this study, the correlation between the amount of modifier dosing and the performance index was used to reflect the applicability of the evaluation index. The greater the correlation, the better the applicability of the index. Among them, the high-temperature performance indexes included failure temperature, softening point, R , J_{nr} and Brookfield viscosity at 135 °C. The specific calculation results are listed in Table 15. The correlation coefficients revealed a good linear relationship between the SPUA modifier admixture and each high-temperature performance index. Among them, the correlation coefficients of apparent viscosity at 135 °C, J_{nr} at two loading levels and R at 3.2 kPa were greater than 0.9, while the correlations of softening point, failure temperature and R at 0.1 kPa were relatively low. This expressed that the apparent viscosity and MSCR tests are more sensitive to the viscoelastic properties of asphalt binders and can evaluate the effect of modifier admixture on the high-temperature properties of asphalt binders more precisely. Therefore, it was recommended to use a Brookfield viscosity test (such as 135 °C) and MSCR test (R and J_{nr}) as the evaluation index of high-temperature performance of the SPMA.

Similarly, correlations between several fatigue performance indices of modified asphalt binders and modifier admixtures were calculated, as shown in Table 16. It can be found that all four fatigue lives showed good linear relationships with the modifier dosing. The correlation between the fatigue life and modifier dose obtained from the LAS test was greater than 0.85, while the correlation between the fatigue life N_{p50} and N_{p20} obtained from the TS test was 0.84 and 0.85, respectively. This indicated that the LAS test was more suitable as a means to evaluate the fatigue performance of asphalt binder characterization.

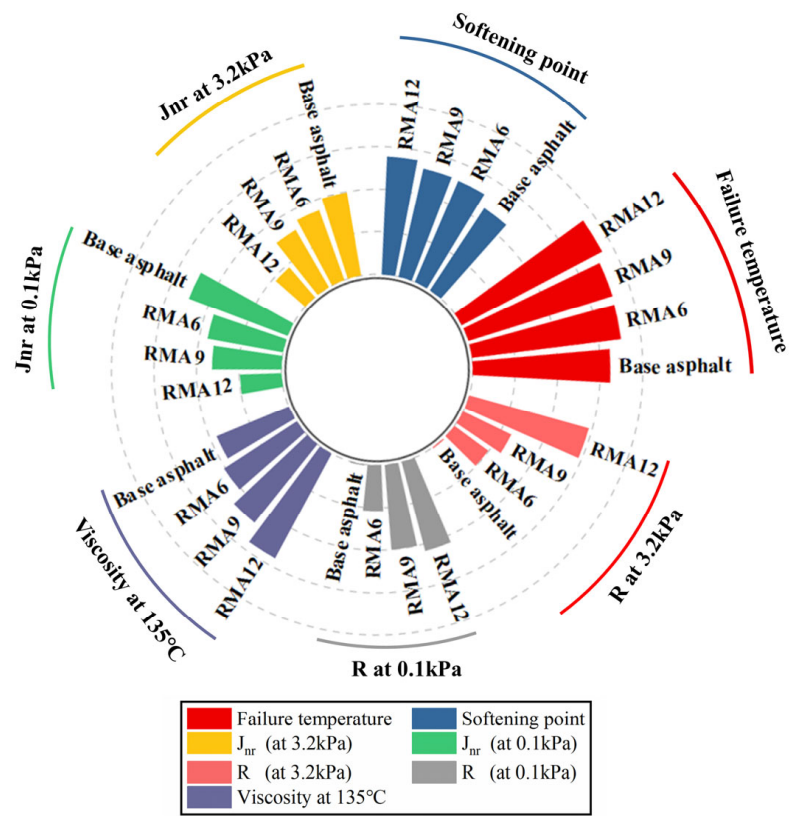


Figure 20. High-temperature performance index of asphalt binders.

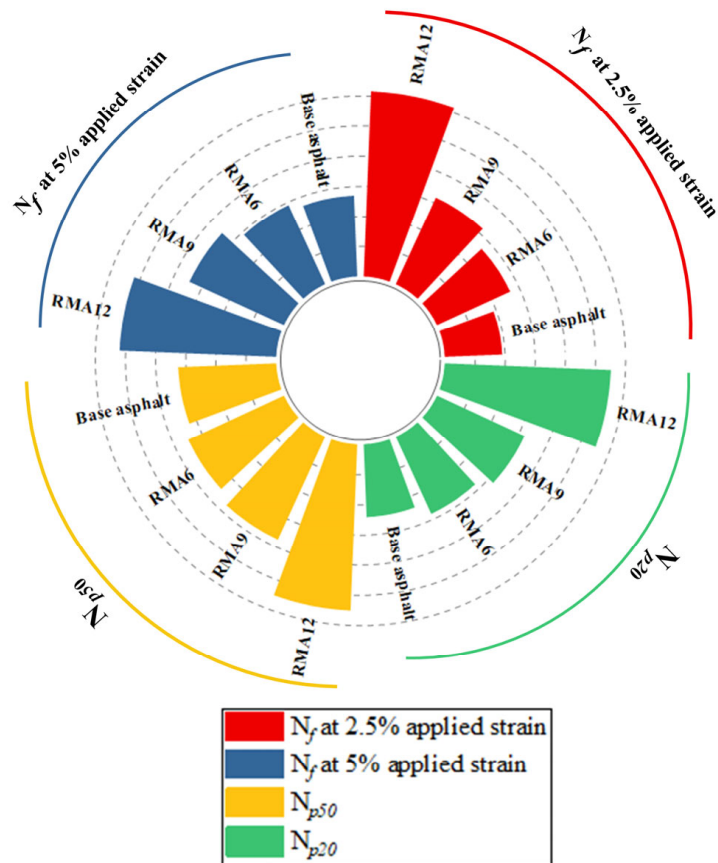


Figure 21. Fatigue Performance index of asphalt binders.

Table 15. Standard deviation of high-temperature index.

High-Temperature Index	Slope	Intercept	Correlation Coefficient
Failure temperature	65.2	66.242	0.81
Softening point	61.7	47.62	0.83
Viscosity at 135 °C	2533.3	252.33	0.99
J _{nr} (at 0.1 kPa)	−2725.0	527.1	0.91
J _{nr} (at 3.2 kPa)	−2750.0	542.6	0.90
R (at 0.1 kPa)	13.9	0.14	0.83
R (at 3.2 kPa)	0.8	−0.005	0.93

Table 16. Standard deviation of high-temperature index.

Fatigue Index	Slope	Intercept	Correlation Coefficient
N _f at 2.5% applied stress	12,767	135	0.91
N _f at 5% applied stress	116,283	−2458.2	0.86
N _{p50}	13,400	494	0.84
N _{p20}	11,283	−55.9	0.85

3.5. Thermal Properties Analysis

Figures 22 and 23 are the result of DSC test. It can be seen from the figure that the overall trend of DSC curves of base asphalt binder and three kinds of modified asphalt was basically the same. The DSC curves and thermodynamic parameters between base asphalt binder and modified asphalt binders had obvious changes. Compared with the base asphalt binder, the DSC curves of the SPMA6 moved up significantly, and the peak temperature rose from 26.3 °C of the base asphalt binder to 38.5 °C, the peak range from 13.2–40.4 °C to 29.3–48.6 °C and the enthalpy change decreased from 10.1 J/g of the base asphalt binder to 2.18 J/g. When the content was 9%, the DSC curve moved up again to a certain extent, but its thermodynamic parameters were almost the same as those of 6% modified asphalt binder. When the modifier content reached 12%, the DSC curve and thermodynamic parameters changed obviously again, the DSC curve moved up, the peak temperature of the endothermic peak further increased and the enthalpy change decreased.

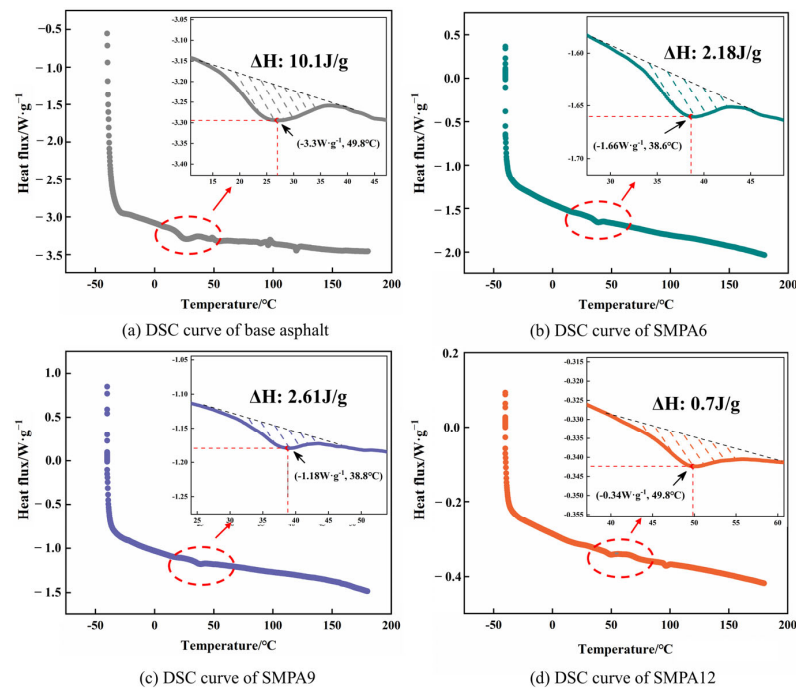


Figure 22. Thermodynamic parameters of asphalt binders.

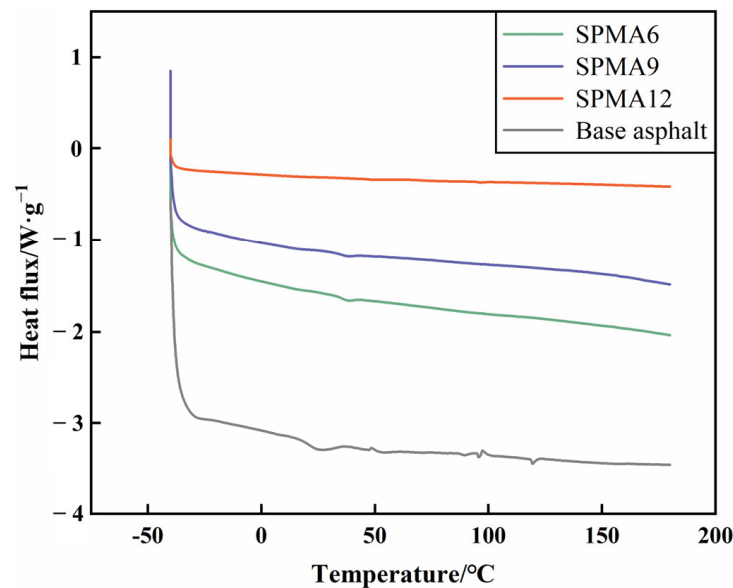


Figure 23. DSC curve of asphalt binders.

This showed that the modifier had a significant effect on the thermal stability of asphalt binders [36]. When the modifier was added, the thermal stability of the corresponding modified asphalt binder was significantly improved. This meant that higher temperature was needed in the process of aggregation transformation in SPUA modified asphalt binder during heating; that is, more energy was needed to complete the transformation of the asphalt phase. The macroscopic performance was improvement in temperature stability of modified asphalt. This explained why SPUA-modified asphalt binder had higher high-temperature performance.

4. Conclusions

The purpose of this study was to evaluate the effect of SPUA as the modifier on asphalt binders. First, the optimum process parameters of the modified asphalt binder were determined based on the orthogonal test. On this basis, by changing the amount of modifier in the asphalt binder, the high-temperature and fatigue properties of the asphalt binder were tested and the applicability of each index to the modified asphalt binder was analyzed. According to the limited experimental results obtained in this study, the following conclusions can be drawn:

- (1) Combined with extreme difference analysis and ANOVA, the best preparation process parameters of modified asphalt binder under the condition of 9% content were determined as follows: shear time, rate and temperature of 40 min, 6000 rpm and 150 °C, respectively.
- (2) The SPUA enhanced the apparent viscosity and improved the high-temperature shear resistance while reducing the temperature sensitivity in the test temperature range.
- (3) Addition of SPUA admixture had a positive effect on high-temperature deformation resistance and elastic recovery performance of asphalt binders but hurt temperature sensitivity. There was higher sensitivity of the MSCR test to the viscoelastic properties of asphalt binders compared to the PG test.
- (4) Increasing the modifier admixture could promote the modifier's effect on fatigue resistance of asphalt binders, but this was detrimental to stress sensitivity of asphalt binders.
- (5) The performance indexes obtained from the MSCR test, Brookfield viscosity and LAS test were more correlated with modifier dosage. Therefore, the MSCR test and Brookfield viscosity test were recommended to evaluate high-temperature performance of asphalt binders and the LAS test to evaluate fatigue resistance of asphalt binders.

- (6) The SPUA modifier had a positive effect on thermal stability of asphalt binders, and the effect increased with an increase in dosage. Higher thermal stability corresponded to better high-temperature performance.
- (7) Excellent high-temperature performance and fatigue resistance of SPMA showed that SPUA material has great potential and application value in asphalt pavement.

Author Contributions: Conceptualization, X.S. Methodology, X.S.; Software, Z.L. and H.Y.; Validation, Z.L. and Y.Y.; Data curation, J.J.; Writing—original draft, Q.P.; Writing—review & editing, Q.P.; Visualization, Q.P. All authors have read and agreed to the published version of the manuscript.

Funding: This paper describes research activities mainly requested and supported by the open research fund of Highway Engineering Key Laboratory of Sichuan Province, Southwest Jiaotong University under grant numbers HEKLS2022-08, by supported by the Fundamental Research Funds for the Central Universities under grant number 300102212516, supported by Open Fund of National Engineering Research Center of Highway Maintenance Technology (Changsha University of Science & Technology) kfj220104, supported by Special Fund for Science and Technology Innovation Strategy of Guangdong Province under grant numbers pdjh2021a0149 and pdjh2022b0161. The sponsorship and interest are gratefully acknowledged, supported by the Key Laboratory of Transport Industry of Road Structure and Material (Research Institute of Highway, Ministry of Transport), Beijing, PRC), supported by Guangxi Key Laboratory of Road Structure and Materials under grant numbers 2021gxjgckf001.

Institutional Review Board Statement: Not applicable.

Informed Consent Statement: Not applicable.

Data Availability Statement: Not applicable.

Conflicts of Interest: The authors declare no conflict of interest.

References

1. Sun, X.L.; Qin, X.; Liu, Z.S.; Yin, Y.M.; Zou, C.; Jiang, S. New preparation method of bitumen samples for UV aging behavior investigation. *Constr. Build. Mater.* **2020**, *233*, 117278. [[CrossRef](#)]
2. Liu, S.; Jin, J.; Yu, H.; Gao, Y.; Du, Y.; Sun, X.; Qian, G. Performance enhancement of modified asphalt via coal gangue with microstructure control. *Constr. Build. Mater.* **2023**, *367*, 130287. [[CrossRef](#)]
3. Wang, C.; Li, Y.; Wen, P.; Zeng, W.; Wang, X. A comprehensive review on mechanical properties of green controlled low strength materials. *Constr. Build. Mater.* **2022**, *363*, 129611. [[CrossRef](#)]
4. Yang, X.; Tang, H.; Cai, X.; Wu, K.; Huang, W.; Zhang, Q.; Li, H. Evaluating reclaimed asphalt mixture homogeneity using force chain transferring stress efficiency. *Constr. Build. Mater.* **2023**, *365*, 130050. [[CrossRef](#)]
5. Yao, X.G.; Li, C.; Xu, T. Multi-scale studies on interfacial system compatibility between asphalt and SBS modifier using molecular dynamics simulations and experimental methods. *Constr. Build. Mater.* **2022**, *346*, 128502. [[CrossRef](#)]
6. Liang, M.; Liang, P.; Fan, W.Y.; Qian, C.D.; Xin, X.; Shi, J.T.; Nan, G. Thermo-rheological behavior and compatibility of modified asphalt with various styrene-butadiene structures in SBS copolymers. *Mater. Des.* **2015**, *88*, 177–185. [[CrossRef](#)]
7. Siddig, E.; Feng, C.P.; Ming, L.Y. Effects of ethylene vinyl acetate and nanoclay additions on high-temperature performance of asphalt binders. *Constr. Build. Mater.* **2018**, *169*, 276–282. [[CrossRef](#)]
8. Brasileiro, L.; Moreno-Navarro, F.; Martínez, R.; Sol-Sánchez, M.; Matos, J.; Rubio-Gámez, M. Study of the feasibility of producing modified asphalt bitumens using flakes made from recycled polymers. *Constr. Build. Mater.* **2019**, *208*, 269–282. [[CrossRef](#)]
9. Celauro, C.; Bosurgi, G.; Sollazzo, G.; Ranieri, M. Laboratory and in-situ tests for estimating improvements in asphalt concrete with the addition of an LDPE and EVA polymeric compound. *Constr. Build. Mater.* **2019**, *196*, 714–726. [[CrossRef](#)]
10. Chen, Q.; Wang, C.; Li, Y.; Feng, L.; Huang, S. Performance development of polyurethane elastomer composites in different construction and curing environments. *Constr. Build. Mater.* **2023**, *365*, 130047. [[CrossRef](#)]
11. Sun, X.; Ou, Z.; Xu, Q.; Qin, X.; Guo, Y.; Lin, J.; Yuan, J. Feasibility analysis of resource application of waste incineration fly ash in asphalt pavement materials. *Environ. Sci. Pollut. Res.* **2023**, *30*, 5242–5257. [[CrossRef](#)] [[PubMed](#)]
12. Sun, X.; Peng, Q.; Zhu, Y.; Jin, J.; Xu, J.; Yin, Y.; Ng, A.H.M. Modification and enhancing effect of SPUA material on asphalt binder: A study of viscoelastic properties and microstructure characterization. *Case Stud. Constr. Mater.* **2023**, *18*, e01781. [[CrossRef](#)]
13. Zhu, H.J.; Wang, X.; Wang, Y.T.; Ji, C.; Wu, G.; Zhang, L.; Han, Z.Y. Damage behavior and assessment of polyurea sprayed reinforced clay brick masonry walls subjected to close-in blast loads. *Int. J. Impact Eng.* **2022**, *167*, 104283. [[CrossRef](#)]
14. Liu, Z.C.; Wu, J.; Yu, J.; Xu, S.L. Damage assessment of normal reinforced concrete panels strengthened with polyurea after explosion. *Case Stud. Constr. Mater.* **2022**, *17*, e01695. [[CrossRef](#)]

15. Liu, Q.; Guo, B.Q.; Chen, P.W.; Su, J.J.; Arab, A.; Ding, G.; Yan, G.H.; Jiang, H.Y.; Guo, F. Investigating ballistic resistance of CFRP/polyurea composite plates subjected to ballistic impact. *Thin Walled Struct.* **2021**, *166*, 108111. [[CrossRef](#)]
16. Ameri, M.; Seif, M.; Abbasi, M.; Molayem, M.; KhavandiKhiavi, A. Fatigue performance evaluation of modified asphalt binder using of dissipated energy approach. *Constr. Build. Mater.* **2017**, *136*, 184–191. [[CrossRef](#)]
17. Wen, Y.K.; Guo, N.S.; Wang, L.; Jin, X.; Li, W.; Wen, H.F. Assessment of various fatigue life indicators and fatigue properties of rock asphalt composite. *Constr. Build. Mater.* **2021**, *289*, 123147. [[CrossRef](#)]
18. Gao, J.F.; Wang, H.N.; Liu, C.C.; Ge, D.D.; You, Z.P.; Yu, M. High-temperature rheological behavior and fatigue performance of lignin modified asphalt binder. *Constr. Build. Mater.* **2020**, *230*, 117063. [[CrossRef](#)]
19. Sun, X.; Zhang, Y.; Peng, Q.; Yuan, J.; Cang, Z.; Lv, J. Study on adaptability of rheological index of nano-PUA-modified asphalt based on geometric parameters of parallel plate. *Nanotechnol. Rev.* **2021**, *10*, 1801–1811. [[CrossRef](#)]
20. Du, Y.; Xu, L.; Deng, H.B.; Deng, D.; Ma, C.; Liu, W.D. Characterization of thermal, high-temperature rheological and fatigue properties of asphalt mastic containing fly ash cenosphere. *Constr. Build. Mater.* **2020**, *233*, 117345. [[CrossRef](#)]
21. Sun, X.L.; Qin, X.; Liu, Z.S.; Yin, Y.; Jiang, S.; Wang, X. Applying feasibility analysis and catalytic purifying potential of novel modifying agent used in asphalt pavement materials. *Constr. Build. Mater.* **2020**, *245*, 118467. [[CrossRef](#)]
22. Li, B.; Liu, P.; Zhao, Y.; Li, X.; Cao, G. Effect of graphene oxide in different phases on the high temperature rheological properties of asphalt based on grey relational and principal component analysis. *Constr. Build. Mater.* **2023**, *362*, 129714. [[CrossRef](#)]
23. Li, Y.; Hao, P.; Zhao, C.; Ling, J.; Wu, T.; Li, D.; Liu, J.; Sun, B. Anti-rutting performance evaluation of modified asphalt binders: A review. *J. Traffic Transp. Eng.* **2021**, *8*, 339–355. [[CrossRef](#)]
24. Cao, W.; Wang, C. Fatigue performance characterization and prediction of asphalt binders using the linear amplitude sweep based viscoelastic continuum damage approach. *Int. J. Fatigue* **2019**, *119*, 112–125. [[CrossRef](#)]
25. Wang, C.; Zhang, H.; Castorena, C.; Zhang, J.; Kim, Y. Identifying fatigue failure in asphalt binder time sweep tests. *Constr. Build. Mater.* **2016**, *121*, 535–546. [[CrossRef](#)]
26. Kim, H.; Mazumder, M.; Lee, S.-J.; Lee, M.-S. Characterization of recycled crumb rubber modified binders containing wax warm additives. *J. Traffic Transp. Eng.* **2018**, *5*, 197–206. [[CrossRef](#)]
27. Zhang, J.; Huang, W.; Zhang, Y.; Yan, C.; Lv, Q.; Guan, W. Evaluation of the terminal blend crumb rubber/SBS composite modified asphalt. *Constr. Build. Mater.* **2021**, *278*, 122377. [[CrossRef](#)]
28. Hong, Z.; Yan, K.; Wang, M.; You, L.; Ge, D. Low-density polyethylene/ethylene–vinyl acetate compound modified asphalt: Optimal preparation process and high-temperature rheological properties. *Constr. Build. Mater.* **2022**, *314*, 125688. [[CrossRef](#)]
29. Xu, C.; Zhang, Z.; Zhao, F.; Liu, F.; Wang, J. Improving the performance of RET modified asphalt with the addition of polyurethane prepolymer (PUP). *Constr. Build. Mater.* **2019**, *206*, 560–575. [[CrossRef](#)]
30. Lei, L.; Li, D.; Chen, Y.; Tian, Y.; Pei, J. Dynamic chemistry based self-healing of asphalt modified by diselenide-crosslinked polyurethane elastomer. *Constr. Build. Mater.* **2021**, *293*, 123480.
31. Wang, Z.; Ye, F. Experimental investigation on aging characteristics of asphalt based on rheological properties. *Constr. Build. Mater.* **2020**, *231*, 117158. [[CrossRef](#)]
32. Dong, R.; Zhao, M.; Xia, W.; Yi, X.; Dai, P.; Tang, N. Chemical and microscopic investigation of co-pyrolysis of crumb tire rubber with waste cooking oil at mild temperature. *Waste Manag.* **2018**, *79*, 516–525. [[CrossRef](#)] [[PubMed](#)]
33. Jiang, X.; Li, P.; Ding, Z.; Yang, L.; Zhao, J. Investigations on viscosity and flow behavior of polyphosphoric acid (PPA) modified asphalt at high temperatures. *Constr. Build. Mater.* **2019**, *228*, 116610. [[CrossRef](#)]
34. Neda, K.; Ataollah, S.; Mousavi, R. Rheological behavior of asphalt binders and fatigue resistance of SMA mixtures modified with nano-silica containing RAP materials under the effect of mixture conditioning. *Constr. Build. Mater.* **2021**, *303*, 124433.
35. Yongjun, M.; Chaoliang, G.; Qixiong, Z.; Yue, Q.; Weikang, K.; Liupeng, F. Study on multiple Damage-Healing properties and mechanism of laboratory simulated recycled asphalt binders. *Constr. Build. Mater.* **2022**, *346*, 128468.
36. Xiaolong, S.; Qin, X.; Guotao, F.; Yongqiang, Z.; Zhengbing, Y.; Qian, C.; Junshen, Y. Effect Investigation of Ultraviolet Ageing on the Rheological Properties, Micro-Structure, and Chemical Composition of Asphalt Binder Modified by Modifying Polymer. *Adv. Mater. Sci. Eng.* **2022**, *2022*, 7190428.
37. Bo, L.; Yufan, C.; Fang, L.; Jianlong, Z. Evaluation of rheological and aging behavior of modified asphalt based on activation energy of viscous flow. *Constr. Build. Mater.* **2022**, *321*, 126347.
38. Hazim, A.-S.; Haryati, Y.; Mohd, S.; Khleel, S.; Putra, J.; Norazah, B.; Radhi, R.; Abdul, H.N. Effects of maltene on the attributes of reclaimed asphalt pavement: Performance optimization. *Constr. Build. Mater.* **2021**, *302*, 124210.
39. Ming, L.; Zhengmei, Q.; Xuehao, L.; Cong, Q.; Ning, G.; Zhaoxin, L.; Linping, S.; Zhanyong, Y.; Jizhe, Z. The Effects of Activation Treatments for Crumb Rubber on the Compatibility and Mechanical Performance of Modified Asphalt Binder and Mixture by the Dry Method. *Front. Mater.* **2022**, *9*, 845718.
40. Li, P.; Jiang, X.; Ding, Z.; Zhao, J.; Shen, M. Analysis of viscosity and composition properties for crumb rubber modified asphalt. *Constr. Build. Mater.* **2018**, *169*, 638–647. [[CrossRef](#)]
41. Xu, X.; Guo, H.; Wang, X.; Zhang, M.; Wang, Z.; Yang, B. Physical properties and anti-aging characteristics of asphalt modified with nano-zinc oxide powder. *Constr. Build. Mater.* **2019**, *224* (Suppl. 1), 732–742. [[CrossRef](#)]
42. Ashish, P.K.; Singh, D.; Bohm, S. Evaluation of rutting, fatigue and moisture damage performance of nanoclay modified asphalt binder. *Constr. Build. Mater.* **2016**, *113*, 341–350. [[CrossRef](#)]

43. Han, L.; Qingshan, X.; Haibo, D.; Hong, Z.; Yanjun, Q. Rheological properties of model wax doped asphalt binders. *Constr. Build. Mater.* **2022**, *350*, 128865.
44. Jiang, J.; Zhao, Y.; Lu, G.; Dai, Y.; Ni, F.; Dong, Q. Effect of binder film distribution on the fatigue characteristics of asphalt Binder/Filler composite based on image analysis method. *Constr. Build. Mater.* **2020**, *260*, 119876. [[CrossRef](#)]
45. Daryoosh, D.; Mahdi, H.; Saqib, G.; Shane, U.B. Combined effect of waste polymer and rejuvenator on performance properties of reclaimed asphalt binder. *Constr. Build. Mater.* **2021**, *268*, 121059.
46. Kumar, D.A.; Dharamveer, S. Evaluation of fatigue performance of asphalt mastics composed of nano hydrated lime filler. *Constr. Build. Mater.* **2020**, *269*, 121322.

Disclaimer/Publisher's Note: The statements, opinions and data contained in all publications are solely those of the individual author(s) and contributor(s) and not of MDPI and/or the editor(s). MDPI and/or the editor(s) disclaim responsibility for any injury to people or property resulting from any ideas, methods, instructions or products referred to in the content.